The Intra-Americas Sea Low-level Jet

Overview and Future Research

Jorge A. Amador

Center for Geophysical Research and School of Physics, University of Costa Rica, San Jose, Costa Rica

A relevant climate feature of the Intra-Americas Sea (IAS) is the low-level jet (IALLJ) dominating the IAS circulation, both in summer and winter; and yet it is practically unknown with regard to its nature, structure, interactions with mid-latitude and tropical phenomena, and its role in regional weather and climate. This paper updates IALLJ current knowledge and its contribution to IAS circulation–precipitation patterns and presents recent findings about the IALLJ based on first *in situ* observations during Phase 3 of the Experimento Climático en las Albercas de Agua Cálida (ECAC), an international field campaign to study IALLJ dynamics during July 2001. Nonhydrostatic fifth-generation Pennsylvania State University National Center for Atmospheric Research Mesoscale Model (MM5) simulations were compared with observations and reanalysis. Large-scale circulation patterns of the IALLJ northern hemisphere summer and winter components suggest that trades, and so the IALLJ, are responding to land–ocean thermal contrasts during the summer season of each continent. The IALLJ is a natural component of the American monsoons as a result of the continent's approximate north–south land distribution. During warm (cold) El Niño–Southern Oscillation phases, winds associated with the IALLJ core (IALLJC) are stronger (weaker) than normal, so precipitation anomalies are positive (negative) in the western Caribbean near Central America and negative (positive) in the central IAS. During the ECAC Phase 3, strong surface winds associated with the IALLJ induced upwelling, cooling down the sea surface temperature by 1–2 °C. The atmospheric mixed layer height reached 1 km near the surface wind maximum below the IALLJC. Observations indicate that primary water vapor advection takes place in a shallow layer between the IALLJC and the ocean surface. Latent heat flux peaked below the IALLJC. Neither the reanalysis nor MM5 captured the observed thermodynamic and kinematic IALLJ structure. So far, IALLJ knowledge is based on either dynamically initialized data or simulations of global (regional) models, which implies that a more systematic and scientific approach is needed to improve it. The Intra-Americas Study of Climate Processes is a great regional opportunity to address trough field work, modeling, and process studies, many of the IALLJ unknown features.

Key words: **Intra-Americas low-level jet; tropical climate variability; MM5 modeling; El Niño—Southern Oscillation; ENSO**

Introduction

Relatively fast-moving currents of geophysical fluids are not unusual in nature. The West Wind Drift (WWD), an ocean current that moves from west to east encircling Antarctica; the Kuroshio Current, the world's second largest current (after the WWD), an oceanic stream found in the western Pacific Ocean off the east coast of Taiwan and flowing northeastward past Japan; and the Gulf Stream in the Atlantic Ocean are just three samples of somewhat rapid-moving salty water currents. The WWD impedes warm waters from reaching the polar caps, while the other two are

Address for correspondence: Prof. Jorge A. Amador, Ph. D., Director, Centro de Investigaciones Geofísicas, Universidad de Costa Rica, San José, Costa Rica. Voice: +502-22075096; fax: +506-22342703. jorge.amador@ucr.ac.cr

Trends and Directions in Climate Research: Ann. N.Y. Acad. Sci. 1146: 153–188 (2008).
doi: 10.1196/annals.1446.012

important in transporting warm tropical waters northward.

Fast-moving air or jet streams have been known to exist in the atmosphere for decades. The major atmospheric wind currents, the polar and subtropical jet streams, are westerly winds at approximately 10 and 13 km high, respectively, in both the Northern Hemisphere and the Southern Hemisphere. These jets can attain mean wind speeds in the range of 15–20 to 30–35 m s^{-1}, depending on the season and hemisphere. Many jet streams in the Earth's atmosphere are thousands of kilometers long, hundreds of kilometers wide, and several kilometers in depth, and their variability, both in space and time, is significant. In the atmosphere, jets have been observed at different levels, in distinct seasons, and in many regions around the globe. Stensrud[1] discusses in detail the wide range of atmospheric phenomena at lower layers that have been described in the scientific literature as low-level jets (LLJs). In the summer, LLJs usually weaker in strength than the upper jet streams, can form in tropical regions near the top of the boundary layer (BL) or in the lower troposphere. Examples of atmospheric LLJs are the Somali Jet (SJ) in east Africa, a cross-equatorial flow from south to north for which Bunker[2] and Findlater[3] were the first to draw scientific attention to and in the Americas, the Great Planes LLJ (GPLLJ), documented by Hoecker Jr.[4] and later by Bonner,[5] and the LLJ just off the west coast of subtropical South America over the Pacific.[6–8]

In general, the atmospheric jet streams, through a series of convergence–divergence patterns, can strongly influence synoptic-scale weather systems in mid and higher latitudes and in the tropics. The LLJs, as their counterpart in upper levels, are also very relevant to climate.[1] These strong currents also play an important role in the global heat, angular momentum, and kinetic energy budgets.[9,10] In lower levels, the SJ accounts for nearly half the interhemispheric mass transport in the lower troposphere around the world.[2]

The dynamic conditions capable of forming and maintaining (especially at lower levels from breaking up against mixing and dissipative forces) such strong air currents are, in general, quite variable depending on fluid characteristics and on external forcing. Several mechanisms, such as thermal gradients over sloping terrains, planetary boundary layer (PBL) oscillations,[11] and land–surface features, have been proposed to explain LLJs immersed in a dormant environment. Large-scale forcing, such as the coupling of upper jet streams with LLJs, their interaction with convective activity,[12] and the synoptic and subsynoptic-scale environment, have been analyzed to explain observed events of the GPLLJ.[13] In the Americas, some of these jet streams, such as the Gulf of California (GC) LLJ,[14–17] the Chocó jet (CJ) in the eastern tropical Pacific (ETP),[18] and the GPLLJ, have been intensively studied through observations[3,4,16,17,19–21] and numerical studies.[22–24]

Regional or global scale experiments have provided significant ocean, land, and atmospheric data to study the structure and dynamics of some LLJs. Meteorology has benefited from such experiments as the Global Atmospheric Research Program (GARP) in the 1960s and the GARP Atlantic Tropical Experiment (GATE) in the 1970s[25,26]; the latter has particularly benefited meteorology with regards to the interaction between the West Africa (WA) LLJ and easterly waves[27,28] and from advances in the understanding of hurricane processes (formation, structure, and role in the circulation) in the tropical Atlantic.[29] More recently, the North American Monsoon Experiment (NAME), conducted in the summer of 2004,[30,31] provided valuable data to analyze the North American Monsoon System (NAMS), the associated LLJs (GCLLJ and GPLLJ), and the summer precipitation distribution.[32–35]

Although there have been a considerable number of meteorological research programs/field campaigns covering the tropical and subtropical Americas in the last decades, such as GARP (1960s—), GATE (1974), the Global Weather Experiment (1978–1979), the World Ocean Circulation Experiment

(1990–1998), and some regional or local experiments, such as the Atlantic Trade Wind Experiment (1969[36]), the Barbados Oceanographic and Meteorological Experiment (1969[37]), the Venezuelan International Meteorological and Hydrological Experiment (1969, 1972[38]), NAME,[30,31] and the Eastern Pacific Investigation of Climate Processes in the Coupled Ocean–Atmosphere System (2000—[39]), the Caribbean region remains to be one of the less-studied areas in the world, despite its societal importance from impacts of many meteorological and climate systems. The Caribbean is home to more than one hundred million people, many of them living in relatively small island states, some of which are among the poorest in the Americas and the world.

Traveling easterly waves,[40] tropical storms and hurricane activity,[41] convective systems,[42] cold fronts reaching tropical regions,[43,44] the mid-summer drought (MSD; *canícula* or *veranillo*),[45] the warm pools,[46,47] the trades, and an intense LLJ,[48] are just some of the meteorological and or climate features that make this region worth studying in the context of an integrated (observations, modeling, processes studies) research program. In this respect, a group of scientists from countries of the region have been working on a Science and Implementation Plan for the Intra-Americas Study of Climate Processes (IASCLIP), to be executed in the near future within the Variability of the American Monsoon (VAMOS) Climate Variability (CLIVAR) Program.

The Caribbean has a unique environment for a remarkable range of meteorological phenomena, such as easterly waves, hurricanes, temporales (periods of weak to moderate rainfall lasting several days), MSD, cold fronts, trade surges, and northerlies, most of which are very little understood in the context of regional weather and climate. One of the most relevant features of this region, practically unknown with regard to its nature, structure, interaction with other regional phenomena of the tropics and extratropics, or in relation to its role in weather and climate, is a LLJ that dominates the Caribbean circulation, both in summer[48–50] and winter,[51,52] which is called the Intra-Americas Sea (IAS) LLJ (IALLJ). Although some evidence of the existence of a wind maximum near the ocean surface can be inferred from previous work[53] or a jet had been suspected to occur in a nearby area where it is currently observed,[1] there seems to be no scientific reference or documentation of the IALLJ before the work of Amador.[48] The IALLJ is a fast-moving trade wind current over the Caribbean Sea with a jet core in the vicinity of 15°N, 75°W,[48] a distinguishable annual cycle, a considerable east–west extent, a low-level wind maximum generally in excess of 10–11 m s^{-1} near the top of the BL (925 hPa), significant horizontal and vertical wind shears, and associated with convective activity and regional precipitation features.[48–50] The IALLJ is also known to be related to other atmospheric signals, such as El Niño–Southern Oscillation (ENSO) and tropical cyclone activity.[49,50,54] In the last years the IALLJ has been addressed, especially by some IAS investigators, as a key feature in local and regional climate.[17,51,55–66]

The objectives of this paper are then twofold: to update current knowledge about the IALLJ in the context of its contribution to weather and climate in the IAS region and present some recent findings about the jet structure and properties based on the first *in situ* meteorological data from field work carried out during Phase 3 of the Experimento Climático en las Albercas de Agua Cálida (ECAC Phase 3) campaign in July 2001 and to compare some results of the observed PBL and lower troposphere structure with fifth-generation Pennsylvania State University National Center for Atmospheric Research (PSU–NCAR) Mesoscale Model (MM5) simulations. This is a unique opportunity since the response of the MM5 BL has been extensively tested over land (Ref. 67 and references therein) but there have been very few studies in which *in situ* observations have been used to evaluate the performance of the MM5 lower layers over the oceans.

In Section 2, the IAS region, as defined in this study, is described. A brief account of the

main topographic features of the IAS is also presented in this section to evaluate the potential role and interaction of complex terrain and the jet characteristics. The data used, a description of the methods used, and the MM5 model configuration are presented in Section 3. The regional and monsoonal circulations relevant to climate of the IAS region and the associated precipitation patterns are briefly discussed in Section 4. Then, an updated review of the known structure, dynamics, and role in weather and climate of the IALLJ is presented, with emphasis on the regional annual and seasonal precipitation distribution. In the next section, two known general circulation models are examined in a very simple way (CCM3.6 and ECHAM4.5) and compared with reanalysis to illustrate errors in capturing the IALLJ. Observations and estimated surface fluxes based on ECAC Phase 3 data during July 2001 are then analyzed to gain some understanding of the Caribbean Sea surface properties under strong wind conditions, as observed during the field campaign. Data from ECAC Phase 3 on the IALLJ structure are compared with reanalysis data[68] to determine to what extent some of the observed LLJ characteristics are captured by these data. This and the MM5 model results are discussed in this section. Conclusions and remarks on future research are finally presented in Section 8.

Physical Features of the Intra-Americas Sea Region

The IAS is defined here as that region consisting of the Gulf of Mexico, the Caribbean Sea, and the ETP adjacent to southern Mexico, Central America, and northwestern South America. Since in general the lands to the west of the Gulf of Mexico and to the east of the ETP are influenced by regional climate features, such as the patterns of the sea surface temperature (SST) associated with the warm pools, the subtropical anticyclones, and trade winds, and by synoptic-scale disturbances coming from the Caribbean Sea and the ETP, these areas are also considered to be part of the IAS, together with northern South America and the state islands in the Caribbean Sea. Figure 1 encloses the area of interest for this study, showing the MM5 model topography. This topography may serve as a reference for the location of the relevant summits and mountains in the continental IAS region (see also DATA and METHODS below for other information drawn in this figure). More details of the region's topography (dominant topographic features) are depicted in the images from NASA's Shuttle Radar Topography Mission (SRTM) for Central America, southern México, and northern South America (available at http://www2.jpl.nasa.gov/srtm/dataprod.htm#Gallery).

The prominent characteristic of southern Mexico and the northern part of Central America is the Sierra Madre del Sur Range with volcanic summits, such as Santo Tomás (3505 m), Atitlán (3537 m), Zunil (3542 m), Agua (3760 m), Fuego (3763 m), Santa María (3772 m), Acatenango (3976 m), Tajumulco (4220 m, the highest in the IAS as defined here) in Guatemala, and Tacana (4092 m) in Mexico. The range spreads east from Mexico between the narrow Pacific plains at the Isthmus of Tehuantepec and the limestone lowland of the Yucatán Peninsula.

Parallel mountain ranges extend across Honduras to the south in Nicaragua where hills decrease in height toward the Managua and Nicaragua Lakes. To the south, the planes extend to northern Costa Rica, defining an important mountain gap from the lowlands of the Mosquitia in Nicaragua and Tortuguero (Costa Rica) on the Caribbean side, to the Papagayo Gulf on the Pacific slope of Costa Rica. The Cordillera Central rises to the south of the northern planes in Costa Rica, reaches the Central Valley with Irazú Volcano (3432 m), and then rises to the Cordillera de Talamanca in Costa Rica with its highest peak Cerro Chirripó (3820 m), before gradually descending to Lake Gatun and the Isthmus of Panama.

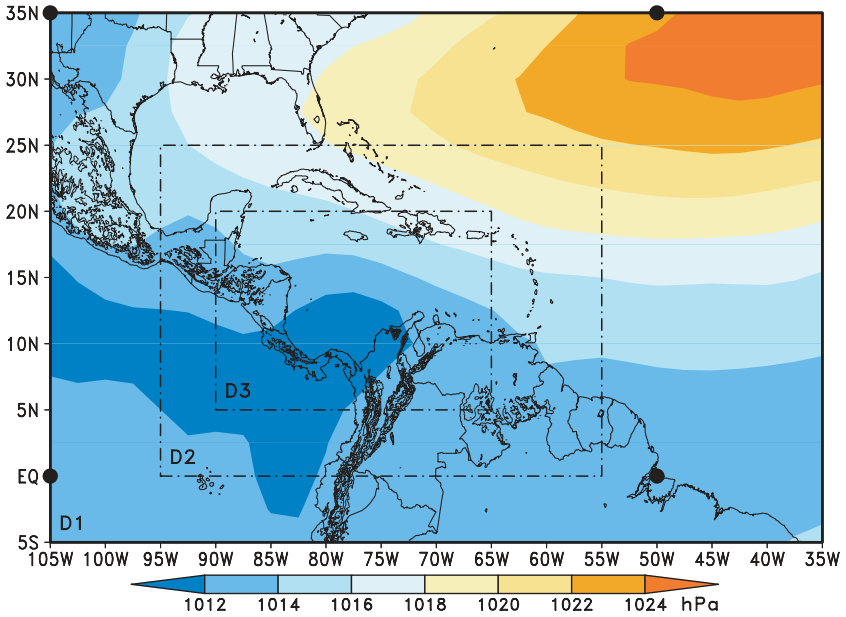

Figure 1. July long-term mean (LTM) sea level pressure in hPa (1958–1999) over the Intra-Americas Sea (IAS) region, as defined here (large black dots). Note the large northeast–southwest pressure gradient over the Caribbean Sea. Also shown in this figure are the fifth-generation Pennsylvania State University National Center for Atmospheric Research Mesoscale Model (MM5) domains with horizontal resolutions of 90, 30, and 10 km (D1, D2, D3, respectively), for the model simulations during Phase 3 of the Experimento Climático en las Albercas de Agua Cálida (ECAC Phase 3) campaign. (In color in *Annals* online.)

In the Caribbean, the highest summit is Pico Duarte (3175 m) in the Dominican Republic. Topographic relief in northern South America is dominated by the Andes Mountains, which extend all along the Pacific Coast. To the east of the Andes and north of the Amazon River, the Guiana Highlands rise in sharp contrast to the surrounding lowlands, indeed hosting the world's tallest waterfall, Angel Falls (979 m). Pico Bolívar in the Sierra Nevada de Mérida is the highest peak in Venezuela (5007 m). On the margin of the Caribbean rises the Sierra Nevada de Santa Marta, an isolated block of mountains composed of a triangular massif of granite whose highest elevation is Pico Cristóbal Colón (5775 m), the tallest peak in Colombia.

The physical features of the IAS and its unique land–sea distribution determine, to a great extent, its mean climate (discussed in Section 4).

Data and Methods

Climatological values of atmospheric parameters were estimated using monthly data from the National Centers for Environmental Prediction/National Center for Atmospheric Research (NCEP/NCAR) reanalysis[68] for the period 1958–1999. QuikSCAT winds (http://manati.orbit.nesdis.noaa.gov/quikscat/; http://winds.jpl.nasa.gov/) and Panamerican Climate Studies/Sounding Network (PACSSONET) data[69] were used to prepare improved spatial and temporal wind fields. Precipitation data used in this study have been described in other works.[45,56] The methods to estimate the monthly deviations of atmospheric parameters and of frequency distributions follow standard procedures. Also, data from ECAC Phase 3[70,71] and climatological values of SSTs[72] were used to study local features associated with the IALLJ over the Caribbean Sea.

Experimento Climático en las Albercas de Agua Cálida

The Climate Experiment over the Americas Warm Pools (ECAC) was aimed at improving the understanding of the elements controlling climate in Mexico, Central America, and the Caribbean. Observations were made in regions with meager information or where no atmospheric data had been collected before. ECAC objectives were, among others,[70,71] to document the atmospheric and oceanic processes related to the MSD,[45] over the northeast Pacific warm pool, and the Caribbean Sea; to examine the air–sea interaction processes over these warm pools that modulate the intensity and distribution of the rainy season on a regional basis, and to make *in situ* sounding observations of the IALLJ during summer over selected regions of the Caribbean. To achieve ECAC's goals, three field campaigns in the northeast Pacific and one in the Caribbean Sea were conducted in 2001. The campaigns in the northeast Pacific warm pool took place during: May 17–27 (ECAC Phase 1), July 7–27 (ECAC Phase 2), and September 1–9 (ECAC Phase 4). In the Caribbean Sea, ECAC Phase 3 was carried out from July 7–27.

Atmospheric observations during ECAC Phase 3 were carried out with twice daily radiosonde launchings from 00.00 UTC July 12 to 00.00 UTC July 25, using Vaisala RS80-15G sondes (Vaisala Oyj, Helsinki, Finland) with Global Positioning System (GPS) tracking (http://www.gps.gov) to derive winds. Standard on-board weather stations (WeatherPak; Coastal Environmental Systems, Inc., Seattle, WA) that included radiation measurements were also used on board the National Autonomous University of Mexico oceanographic research vessel Justo Sierra.[70] Oceanic observations were mostly focused on conductivity, temperature, and depth instrumentation and thermosalinograph (TSG) measurements. Wind speed and direction, temperature, and relative humidity were measured with the WeatherPak station located at 9.5 m above sea level. Bulk SST was determined by a SBE 45 MicroTSG (Sea-Bird Electronics, Inc., Bellevue, WA).

The cruise track had three phases: outbound phase (Tuxpan to Puerto Morelos), main survey (Table 1), and inbound phase (back to Yucatan Channel and Tuxpan). The 10 legs of the main survey (4280 km) were determined by turning points as shown in Table 1 (adapted from the ECAC Phase 3 report[68]).

Relative humidity (i.e., percent saturation) from GPS radiosonde data was converted to specific humidity (i.e., in g kg^{-1} units) in a conventional manner.[73] Sensible and latent heat fluxes (LHF) were estimated using the Coupled Ocean Atmosphere Response Experiment (COARE) bulk air–sea flux algorithm, version 3.0b.[74] The bulk formulation used is an Excel/VBA translation by Greg Pelletier (http://www.ecy.wa.gov/programs/eap/models.html), based on a Fortran77 program (cor3_0bf.for) developed for COARE[72] for a range of wind speed validity from 0–20 m s^{-1} (ftp://ftp.etl.noaa.gov/user/cfairall/bulkalg/cor3_0/). Ship-relative wind speed and direction were converted to absolute (earth-relative) winds using ship navigation data and compass readings.[75] The algorithm used for computing meteorological true winds is available as FORTRAN routines (http://www.coaps.fsu.edu/woce/truewind/).

MM5 Model Configuration

The PSU–NCAR MM5 is a nonhydrostatic, primitive equation, fully compressible atmospheric model.[76] The MM5 has been widely used for mesoscale studies[67,76,77]; it was designed for real-data modeling studies, and most of the previous research with this model has been initialized with observational/objective-analysis data.[67] The MM5 used in this study was configured with nonhydrostatic dynamics, and three nested domains with the outer domain (D1) covering approximately the IAS region. Figure 1 shows the model domains with the approximate regional topography. The model simulations made use of a two-way

TABLE 1. The 10 Legs of Experimento Climático en las Albercas de Agua Cálida (ECAC) Phase 3 Main Survey

	From (°N, °W)		To (°N, °W)		From (July 2001)		To (July 2001)		Distance
Leg	Lat	Lon	Lat	Lon	Day	Local time*	Day	Local time*	(km)
I	21,0	86,7	17,5	78,0	11	07:20	14	12:10	990
II	17,5	78,0	15,0	80,7	14	12:10	15	17:30	398
III	15,0	80,7	13,0	79,8	15	17:30	16	15:25	244
IV	13,0	79,8	15,0	79,5	16	15:25	17	07:55	225
V	15,0	79,5	13,0	79,8	17	07:55	18	02:30	225
VI	13,0	79,1	13,6	78,7	18	02:30	18	12:10	83
VII	13,6	78,7	15,7	80,6	18	12:10	19	14:20	305
VIII	15,7	80,6	19,2	86,4	19	14:20	21	16:40	722
IX	19,2	86,5	21,2	81,1	21	16:40	23	07:45	546
X	21,2	81,1	21,6	85,6	23	07:45	24	08:00	542

*Local time = UTC – 6.

nesting scheme with domains with horizontal resolutions of 90, 30, and 10 km (49 by 86, 94 by 148, 172 by 277 grid points, respectively) and 50 vertical levels, 15 of which were located in the first kilometer above the surface of the model. The inner domain (D3) was centered in the IALLJ core near 15°N, 75°W (Fig. 1). Physical options for all the model simulations are Dudhia's simple ice scheme[77] and Grell's cumulus parameterization.[76] The cloud radiation scheme was selected to account for diurnal variations during the simulation and the Gayno–Seaman scheme was used for the PBL. The model was initialized using reanalysis data[68] from 00.00 UTC July 12, 2001, to 00.00 UTC July 25, 2001, with sounding data assimilation every 12 h from the ECAC Phase 3 campaign.

The next section on climate of the IAS follows basically the approach taken by Amador *et al*.[52]

A Brief Summary of Climate of the Intra-Americas Sea Region

Regional and Monsoonal Circulations

Short-wave radiation coming from the sun and reaching the top of the atmosphere depends upon the earth–sun astronomical parameters, so at any given latitude, the Earth receives variable amounts of radiation throughout the year. Outside the tropics, seasonal radiation changes can be significant. Radiation data for the IAS show that the annual, mean surface, incoming, shortwave radiation flux reaches a maximum near the easternmost part of the ETP that extends along the Central American and southwestern Mexico coasts and also reaches a maximum in the southern parts of the Caribbean Sea near Venezuela, both regions with values in excess of 250 W m^{-2}.[50]

The subtropical highs near lat 30°N [the Azores High (AH) is just seen in the northeastern corner of the IAS in Fig. 1] in both the Pacific Ocean (the North Pacific High) and Atlantic Ocean (also the Bermuda High) and the low pressure belt[78] at low latitudes define a strong meridional pressure gradient between these systems that accelerates the air toward equatorial regions. This moving air is known as trades and is observed as northeasterly winds in the Northern Hemisphere from the Coriolis effect. The trades converge toward low latitudes,[41] carrying moisture south and forcing the air into the Intertropical Convergence Zone (ITCZ), a region of strong upward motion. In a different time-scale frame, the AH has been found to vary in phase with the North Atlantic Oscillation (NAO) and the IALLJ in such a way that strong (weak) AH is associated with a strengthening (weakening) of both the NAO and the jet.[61]

The SST shows a maximum just off the west coast of Central America and southern Mexico most of the year.[52] The seasonal cycle of SST is very important in the IAS since it defines key regional features for climate, especially during the period July–September when the Western Hemisphere warm pool (WHWP) develops,[46,47,79] the MSD appears,[45,80] and cyclogenesis is mostly favored.[81] During the northern winter, SST isotherms over the Caribbean and the eastern tropical Pacific are mostly zonally distributed (with values usually below 28–29 °C),[52] the trade winds are more intense and nearest to the equator during late winter and early spring of the respective hemispheres,[82] and the ITCZ is at its southernmost position.[83]

Cold northerly winds, often referred to as "los nortes"[84] or "northers" appear in most of the IAS region, especially during December–March. These air masses coming from northwest Canada and the polar region penetrate deep into the tropics to produce strong wind events associated with intense rainfall.[43,44] As a consequence of these cold fronts, winds are funneled through mountain passes in southern Mexico and Central America, the Chivela Pass on the Isthmus of Tehuantepec (Tehuantepec wind jet or Tehuantepec Nortes), the central lowlands of Nicaragua and northern Costa Rica (Papagayo wind jet or Papagayos), and the Central Isthmus of Panama (Panama wind jet). The long-term monthly wind speed and frequency of occurrence of "los nortes" at Chivela Pass show a bimodal distribution with maximum values in December–January and July.[85] Cold fronts first cross the Isthmus of Tehuantepec and move southeastward, creating relatively high surface pressure in the southwestern Caribbean Sea. The pressure difference between the Caribbean and Pacific basins triggers strong low-level flow across the Lake of Nicaragua and northern Costa Rica that can extend far into the ETP.[52]

On regional and local scales, the interaction of the predominant trade wind regime with the highly complex topography in some areas of Central America[51] and southern Mexico explains a large percentage of the temporal and spatial rainfall variability over this region, especially at intermediate- and high-elevation sites. Also, diurnal heating and convective activity associated with the ITCZ are important mechanisms that determine precipitation patterns in most of the Caribbean islands and in the coastal regions of Central America and southern Mexico.

On larger scales, monsoonal circulations in the Americas are mostly longitudinally dependent time-averaged motions forced by topography and by oceanic and continental heating contrasts. Two major systems, the NAMS and the South American Monsoon System (SAMS), form part of the American Monsoon System (AMS). Both, NAMS and SAMS exhibit many of the fundamental features of the major monsoon regions of the world.[86] Interaction of the NAMS and SAMS with the trades is a very important factor in explaining warm season precipitation distribution in many regions of the Americas. The NAMS and SAMS have been associated with the summer precipitation of the respective regions,[20,87,88] the latter precipitation amount being considerably greater than the former. Both monsoonal circulations are known to account for more than 50% of total annual precipitation during their respective summer seasons[86] and are responsible for the LLJs. The NAMS has been related to the formation of the southerly GCLLJ[14,15] and the SAMS with the South America LLJ (SALLJ) (Ref. 86 and references therein).

The SAMS exhibits somewhat distinct characteristics compared to the other monsoon systems, given that most of South America is situated in the tropics and seasonal temperature differences are less pronounced than in other subtropical monsoon regimes. A large-scale circulation of the monsoon type develops in the northeastern tropical Pacific during summer,[30] but no clear reversal of the wind is observed during winter in some areas of the IAS (e.g., Central America) to complete the monsoonal cycle, as it is usually defined.[89] A remarkable feature of the IAS is that an LLJ

develops during both the boreal summer[48] and boreal winter.[51,52] The role of the summer and winter components of the IALLJ in the NAMS and SAMS circulations is still unclear, but the patterns of the large-scale circulation suggest that these two components may just be the atmospheric dynamic response to the intense land–sea temperature contrast of the corresponding summer caused by the approximate north–south distribution of land in the Americas.

Considerable debate is still going on about the moisture sources that feed precipitation processes over the monsoonal regions. Although the Gulf of California and the ETP appear to be the logical primary sources of humidity for the monsoon, besides those regions[90] the Gulf of Mexico also contributes to the moisture budget over the NAMS region. A recent work[17] estimated the atmospheric moisture transport over the United States and Mexico using the NCEP regional reanalysis and concluded that regional reanalysis, during the monsoon period, is able to capture important features of the IALLJ and the GPLLJ, which "transport copious moisture from the Caribbean to the Gulf of Mexico and from the Gulf of Mexico to the Great Plains, respectively" (p. 710). In other studies, the summer component of the IALLJ has been confirmed as an important element to carry moisture from the ocean to the central United States.[61,91] Intraseasonal, interannual, and decadal variability of the NAMS has already been summarized,[30] but no relationship has yet been found between the IALLJ and those modes.

Near the South American coasts (north of the equator) the southerly trade wind regime becomes westerly, except in February, because of the change of sign of the Coriolis force and because of the land–sea temperature gradient, among other elements.[41] In western Colombia near 5°N, these winds form a low-level westerly jet, the CJ,[18] with maximum values of 6–8 ms^{-1} near 925 hPa during October–November. At lower levels, warm air and moisture convergence associated with the CJ, low surface pressure, and topographically induced vertical motion on the western Andes contribute to deep convective activity organized as mesoscale convective complexes.[92]

Precipitation

Mesoscale- to synoptic- to global-scale systems hit the IAS region and interact with the regional complex topography and local atmospheric features to determine a large range of multi-scale precipitation variability. Convective activity over the Caribbean Sea and ETP is very much dependent on SST values and atmospheric forcing associated with tropical waves and tropical cyclones. Over land, afternoon heating is the most likely cause of convective activity and associated precipitation on a daily basis. The generation of seasonal precipitation is also associated with the trades in both basins.

The annual rainfall distribution (Fig. 2) shows a marked contrast between the Caribbean and Pacific slopes of Central America and southern Mexico. A bimodal distribution of rainfall predominates on the Pacific side, with maxima in June and September–October and a clear reduction in rainfall during July–August. This decrease in precipitation is known as MSD,[45] although it is not a drought in its own sense. The MSD forms part of the seasonal cycle of precipitation in the region, extends well into the ETP,[43] and has a large interannual variability that is so far not understood. Figure 3 shows the precipitation distribution, as expressed in terms of a variability index (VI), at two meteorological stations (see Table 2 for station information), Barbacoa in Nicaragua (Fig. 3A), and Usulutan in El Salvador (Fig. 3B), both on the Pacific slope of Central America. The VI was calculated as:

$$\mathrm{VI}_{k+1} = \{(P_{k+1} - P_k)/P_{\mathrm{m}}\},$$

where $k = 1, \ldots, M$. M is the total number of months in record in chronological order, P_k is the precipitation for a given month k, and

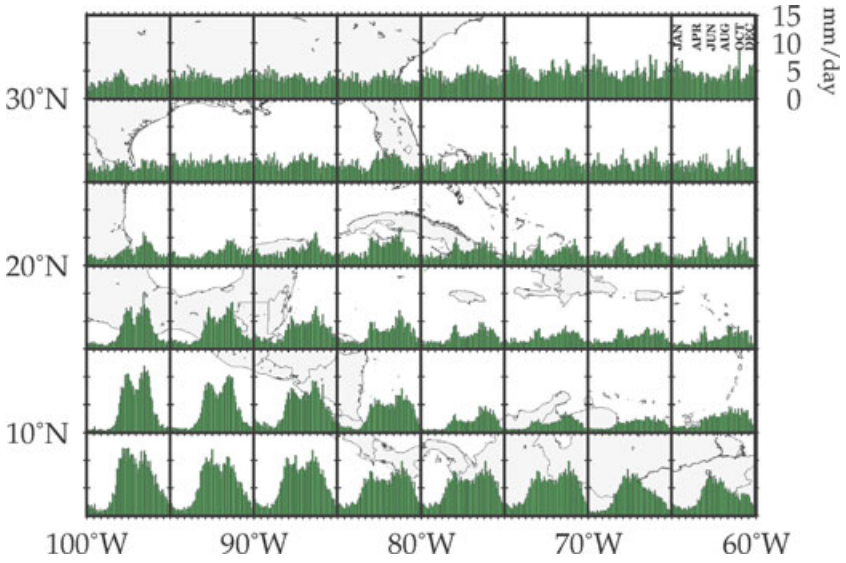

Figure 2. Distribution of climatological 5-day mean precipitation rates (mm day^{-1}) for contiguous $5^\circ \times 5^\circ$ areas.[45,56] Note the bimodal precipitation distribution, especially in the eastern tropical Pacific (ETP), showing the mid-summer drought (MSD), a reduction in rainfall during July–August. (In color in *Annals* online.)

P_m is the mean annual rainfall for the station estimated over the number of years in record. It is noted in both distributions that there is a large interannual variability in the start, duration, and end of the dry and rainy seasons and a noticeable disruption in the rainfall corresponding to the MSD during the summer months (July–August) that also shows a large fluctuation in those time scales. It was hypothesized[43] that changes in the short-wave radiation reaching the ocean surface were associated with the intensity of the convective activity over the eastern Pacific warm pool (EPWP). The evolution of various meteorological parameters that had been related to the occurrence of the MSD in that region partially held during the ECAC field campaigns in the Pacific in the summer of 2001.[71] However, examination of reanalysis SST data in the region showed that SST subseasonal variations are too small in amplitude and spatial coverage to propose that SST be the primary or ultimate cause of the MSD.[93] During this reduction in precipitation, the trade winds over the Caribbean are observed to intensify, in part because of the dynamical response of the low-level atmosphere to the magnitude of the convective forcing in the ITCZ, which in turn is associated with the SST pattern in the EPWP and to the strengthening of the north–south pressure gradient.[52] The relationships between the MSD and its interannual variability with fluctuations in

TABLE 2. Characteristics of the Meteorological Stations Used in this Study

Station	Lat (N)	Lon (W)	Altitude (m)	Period
Liberia	10°36′	85°32′	80	June 7–17, 1997
Managua	12°13′	86°17′	56	July (1900+, 98, 99; 2000+, 00, 01, 02, 04, 05, 07)
				February (1998; 2000+, 01, 02, 05, 07)
				July 1–10, 2000
Barbacoa	12°34′	86°11′	480	(1958–1988)
Usulutan	13°20′	88°26′	75	(1928–1993)

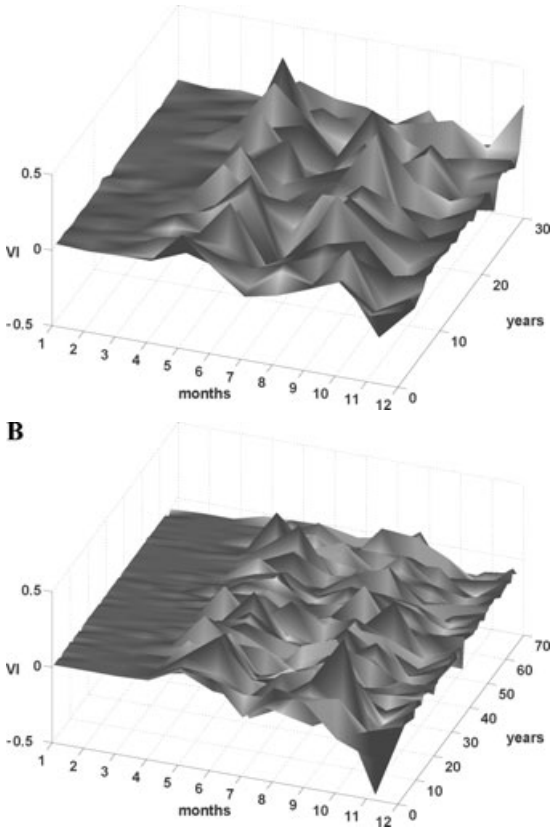

Figure 3. Interannual variability of the mid-summer drought (MSD) at **(A)** Barbacoa in Nicaragua and **(B)** Usulutan in El Salvador, both on the Pacific coast of Central America. The variability index (VI) is defined in the text. Table 2 contains the station characteristics and periods used.

various time scales of the IALLJ or with other large-scale modulators (e.g., El Niño, La Niña) are not known.

From December to March, the Pacific slope of Central America shows mostly dry conditions, and the ITCZ is at its southernmost position. In the Caribbean, precipitation during this period is mostly associated with mid-latitude air intrusions[43,44] and with less frequent low-level cloud systems traveling from the east and reaching the ETP.[94] The boreal winter months along the Caribbean slope of the IAS are more humid than those on the Pacific side.[45] Regarding the onset and end of the rainy season, several studies have presented evidence that fluctuations of the SST of the tropical Atlantic and Pacific Oceans are related to variations in the duration and timing of the wet season in Central America.[95] Fluctuations in the equatorial tropical Pacific and in the tropical north Atlantic/Intra-Americas Sea region also affect precipitation and temperature in Mesoamerica.[93,96–99] The strongest rainfall signal takes place when tropical North Atlantic SST anomalies are in a configuration of meridional dipole (antisymmetric across the ITCZ) and tropical Pacific anomalies are of the opposite sign.[95]

Another type of disturbance that contributes to seasonal precipitation in some parts of the IAS (e.g., Central America) is the "temporales."[41] The name "temporales" is used mostly on the Pacific coasts of Central America for a period of weak-to-moderate nearly continuous rain that can last several days and can affect a relatively large region. The temporales for the Pacific region of Central America have been characterized as having light winds[39]; however, in some cases, winds can be intense and long lasting[51] and may be associated with surges in the trades[51] and the LLJ activity. The occurrence of these events presents a large interannual and intraseasonal variability, and their relationship to ENSO or to other large-scale climatic signals is not clear.

In the intraseasonal modes, precipitation is dominated by the Madden–Julian Oscillation (MJO). In 1972, Madden and Julian[100] called this oscillation the "40–50-day oscillation" because of its preferred time scale. The MJO is characterized by an eastward propagation of deep-convective anomalies over the warm pool regions and involves fluctuations in wind, SST, cloudiness, and rainfall. What is the relationship, if any, between the MJO and the IALLJ?

The Intra-Americas Low-level Jet

Annual Cycle, Intraseasonal and Interannual Variability

The most interesting circulation feature over the Caribbean Sea and Central America during summer and winter is the IALLJ. The jet shows a clear annual cycle (Fig. 4) with two

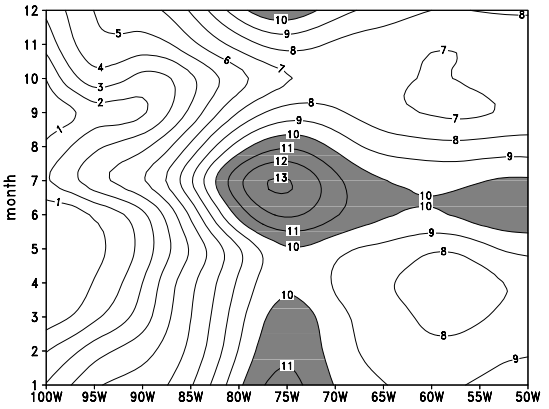

Figure 4. Time–longitude cross section of monthly mean wind speed (m s^{-1}) at 925 hPa averaged from 12.5 to 17.5 °N from reanalysis.[68]

wind maxima near 925 hPa, one in July and the other in January–February.[51,52,62,91,101,102] The first annual peak starts, in general, to develop in early June just after the onset of the rainy season in Central America, reaches a maximum in July, and then weakens in early September.[48–50] As observed in this figure, the jet core seems to extend eastwards beyond 50°W. During September to early November, trades are relatively weak, vertical wind shear over the Caribbean is reduced, hurricane activity peaks, and rainfall spreads almost all over the IAS. In late November or early December, trades increase again, cold surges from mid and high latitudes start to reach the tropics, and the second maximum of wind appears over the Caribbean Sea.[51,52,101,102] The long-term mean (LTM) of the wind vector at 925 hPa (approximately 800 m height) for July and February (1958–1999) is shown in Figure 5A and B, respectively. Winds in excess of 13 ms^{-1} dominate the central Caribbean Sea (15°N, 75°W) in summer where the jet core widens east–west and extends upward to 700 hPa. The winter component of the jet appears to be compressed below 850 hPa with values of up 10 m s^{-1}, with a strong vertical wind shear, an element unfavorable for convection. These differences in the IALLJ component's strength, however, should be taken with caution, since this is an area with scarce meteorological data.

In situ observations taken just north of the mean jet core position at 15°N during a field experiment (ECAC Phase 3 in July 2001) show that, on a daily basis, the vertical structure of the IALLJ with a maximum speed of 10 m s^{-1} or more at about 1000 m above sea level remains well defined (Fig. 17 in Ref. 52). All the dynamic conditions that originate and keep this jet from weakening against dissipative forces or from other atmospheric interactions have yet to be understood. Its barotropically unstable nature was established for the summer of 1991[103] and later for longer time periods,[48] so the IALLJ has potential for interaction with transients, such as the easterly waves traveling over the Caribbean.[40] A recent research work[104] analyzed the interaction between easterly waves and the mean current over the Caribbean for the period May–October 1948–2001, estimating the barotropic energy conversions between these two modes using the Elliassen-Palm flux vector. Results showed that from May to July, easterly waves lose energy and momentum, strengthening the mean current and causing the low-level jet to peak in July. From August to October the IALLJ contributes with momentum to the intensification of the waves, so the jet decreases in intensity, as observed in reanalysis data.[48] The most unstable waves have phase speeds of approximately 6° per day (7 m s^{-1}), reach their maximum intensity at 700 hPa (contrary to African waves that peak at 850 hPa), have wavelengths of a little less than 3000 km, and have periods between 5–7 days.[104] These findings make the IALLJ an important element for explaining convective activity during the second half of the year and contribute to the understanding of regional climate; however, they are obviously not applicable to winter when the IALLJ reaches a peak in February when no major tropical wave activity is observed. The intensification of the trades during boreal winter and the corresponding peak of the IALLJ in February may be from the strengthening of the meridional pressure gradient in the Atlantic and to the thermal contrast between the Caribbean Sea and the SAMS.

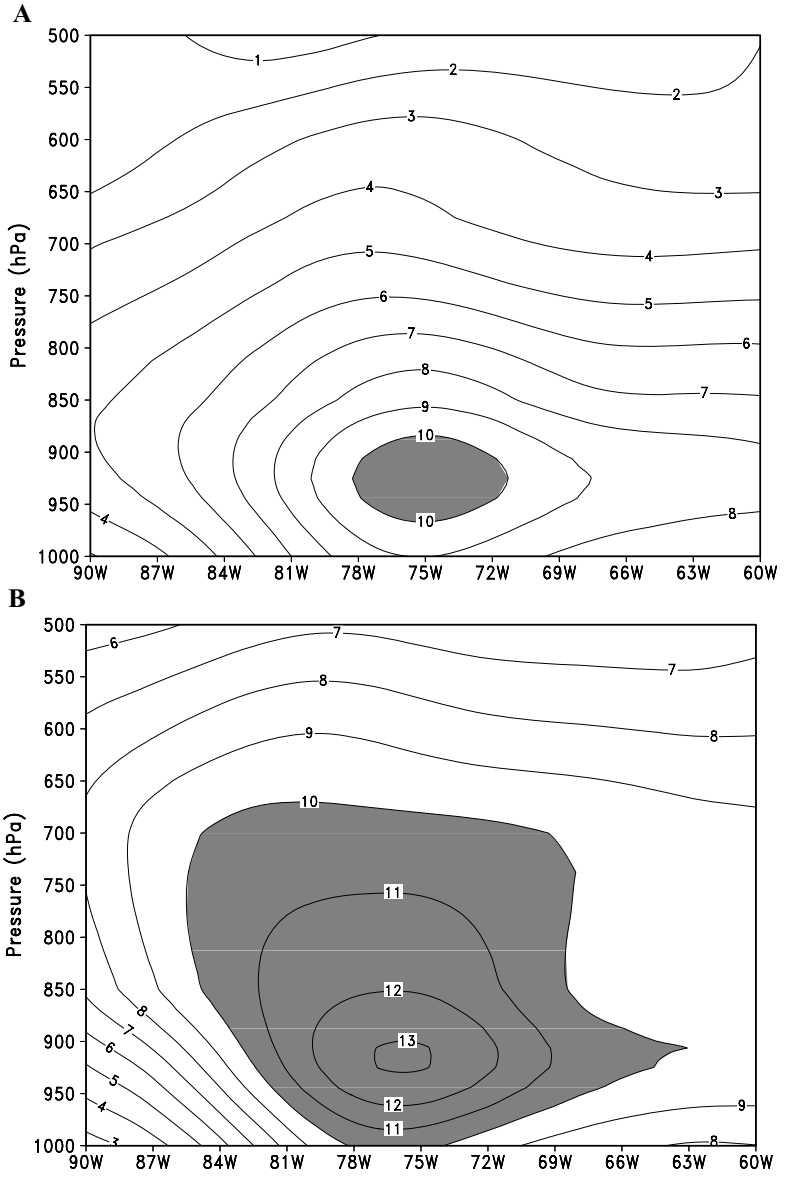

Figure 5. Vertical profile of monthly mean wind speed (m s^{-1}) averaged from 12.5 to 17.5 °N from reanalysis for **(A)** February and **(B)** as in (A) but for July.[68]

The IALLJ crosses Central America through the mountain gaps and reaches the easternmost region of the tropical Pacific.[52,63] Figure 6A and B present low-level mean flow at Managua (Nicaragua) using PACS-SONET data for several distinct periods to illustrate, in the mean, the jet strength over land and into the Pacific for summer and winter, respectively (see Table 2 for station information and periods used). Note that the IALLJ at Managua can be very strong during both July and February with mean values greater than 16 m s^{-1}. In Figure 6 the height of the maximum winds appears to increase from the western Caribbean to Central America and into the Pacific, although there is a lot of vertical fluctuation in the jet core. Figure 7 illustrates the jet structure and some surges associated with synoptic-scale jet events

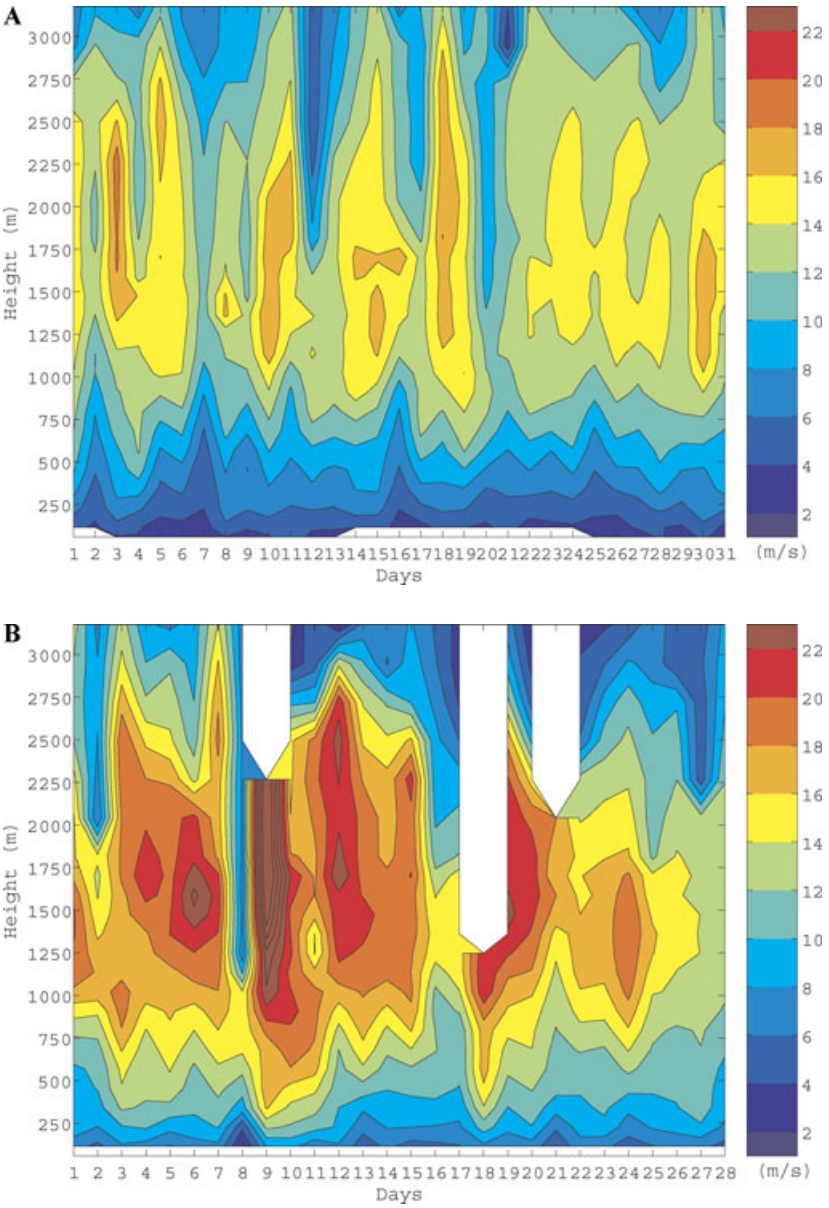

Figure 6. Mean low-level flow (m s^{-1}) at Managua, Nicaragua for **(A)** July and **(B)** February from the Panamerican Climate Studies/Sounding Network (PACS-SONET) data. Table 2 contains the station characteristics and periods used. (In color in *Annals* online.)

at Liberia in northwestern Costa Rica (Fig. 7A) and at Managua (Fig. 7B) for some different short periods (Table 2) that are usually associated with strong wind–topography interaction and precipitation on the Caribbean slope of Central America.[51]

QuikSCAT wind data confirms that low-level flow crosses Central America reaching the Pacific Ocean in both boreal summer and boreal winter (Fig. 8A, B, respectively). This strong current is different from what has been termed the *Papagayo jet*, a winter feature that has been proposed as the forcing mechanism for the Costa Rica dome.[105–107] There is a striking difference in the flow configuration for summer and winter in Figure 8. During

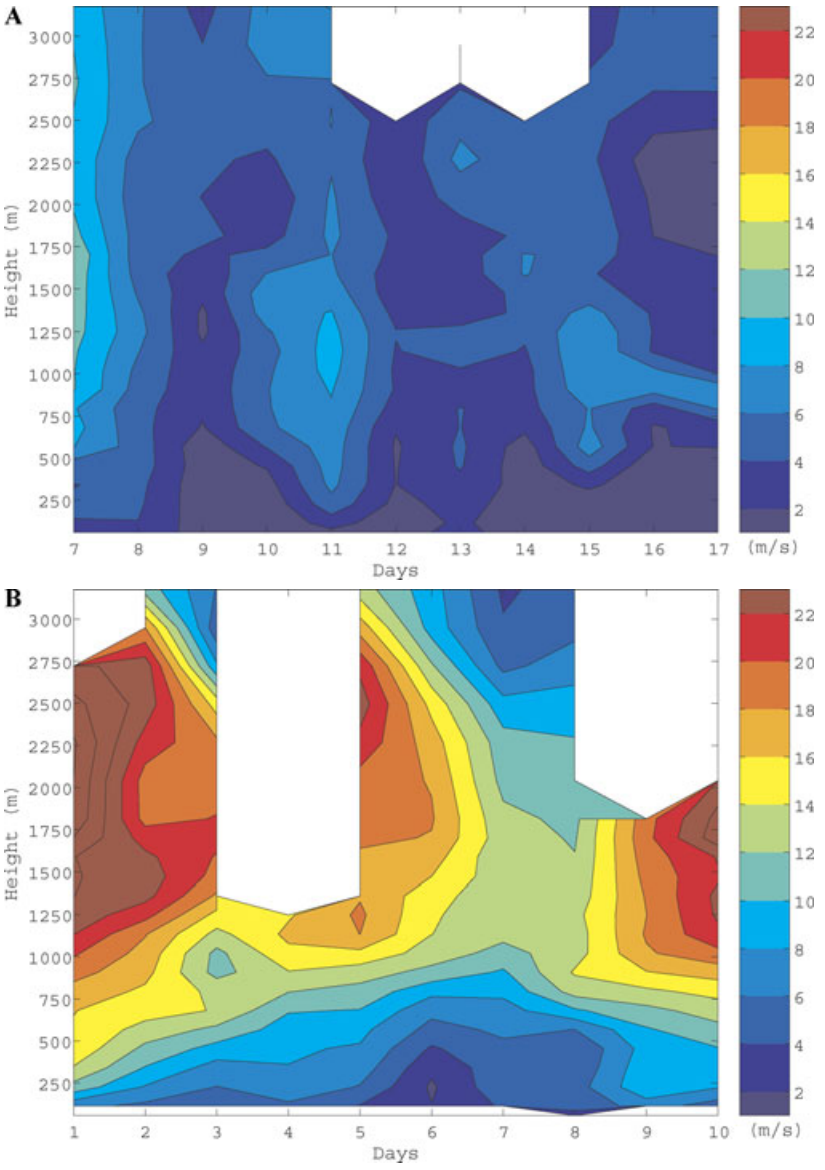

Figure 7. Low-level flow (m s^{-1}) at **(A)** Liberia, Costa Rica, for the period June 7–17, 1997, and **(B)** Managua, Nicaragua for the period July 1–10, 2000, from PACS-SONET data. Table 2 contains the station characteristics. (In color in *Annals* online.)

the northern summer, the LLJ splits in two branches as it passes over the Caribbean, one branch turns toward the north and the other crosses Central America and continues into the Pacific; whereas for winter, the IALLJ turns south, at the entrance of the South American subcontinent and after crossing the Central American land bridge. This large-scale circulation pattern suggests that trades, and so the IALLJ, are responding to thermal contrasts during the summer season of the corresponding subcontinent, and it is a natural component of the AMS. This IALLJ annual behavior may also be associated with the approximate north–south distribution of land in the Americas, which is in turn related to north–south thermal contrasts, especially during the corresponding subcontinent summer season. Since

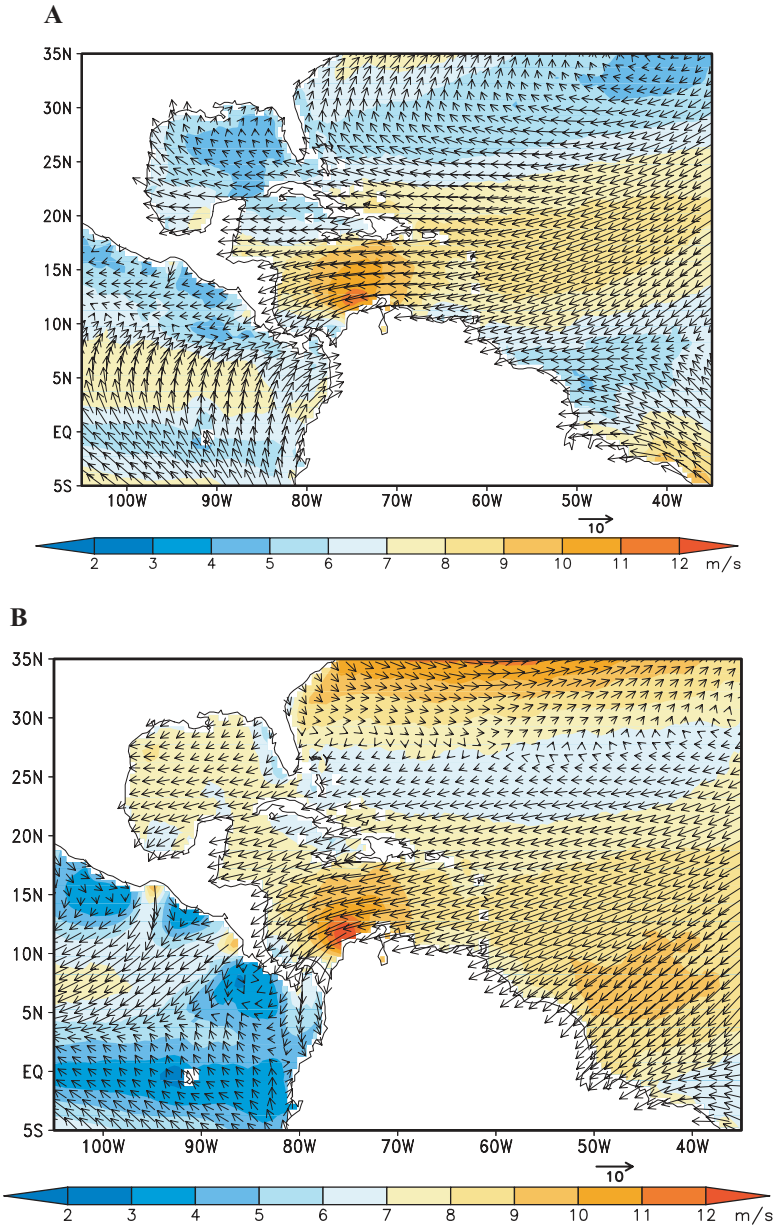

Figure 8. Mean QuikSCAT winds (m s^{-1}) for **(A)** July and **(B)** February for the period 2000–2007. (In color in *Annals* online.)

the IALLJ core intensity varies with ENSO phases in such a way that during warm (cold) events the jet core is stronger (weaker) than normal in the boreal summer, surface wind stress and wind stress curl are expected to be stronger (weaker) than in normal years in the easternmost portion of the ETP. Contrary to what happens in summer, the jet core is weaker (stronger) than normal during warm (cold) ENSO phases in winter.[51,52] Also, strong surface winds associated with this LLJ offshore the Gulf of Papagayo influence SST over the ETP[108] and probably the Costa Rica dome dynamics.

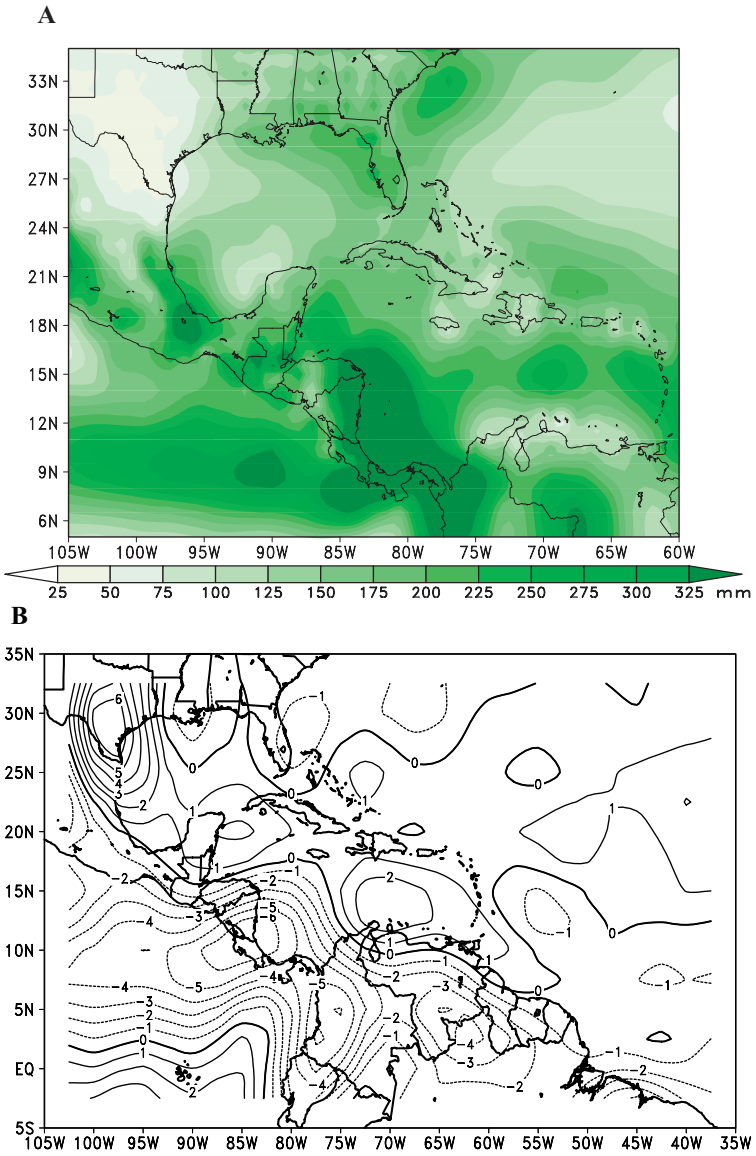

Figure 9. (A) Precipitation (mm) distribution for July (CRN073 data[45,56]) and **(B)** pattern of wind divergence–convergence (10^{-6} s^{-1}) at 925 hPa for July from reanalysis.[68] (In color in *Annals* online.)

The Large-scale Environment and the IALLJ Role in Regional Weather and Climate

Figure 9A presents the precipitation distribution for the IAS for July, and Figure 9B shows the divergence–convergence fields at 925 hPa. As can be noted from this figure, the precipitation maximum is located where there is strong large-scale convergence of the wind field, which in turn coincides with the jet exit at lower levels.[48–50,52,109] At the jet entrance near the core (approximately 65°W), as expected from basic principles, a region of divergence dominates the Caribbean. Where low-level divergence is detected (northern Venezuela and eastern Caribbean), precipitation is scarce. Also, cooling from coastal upwelling induced by the

jet might contribute to the semi-arid regions of northern Venezuela and the Netherlands Antilles.[110] In intraseasonal time scales, changes in the low-level circulation over the Caribbean and the eastern North Pacific explain variations in the evolution of the rainy season over Mexico.[55]

Although topography is highly complex in southern Mexico, Central America, and northern South America, the precipitation maximum in Figure 9A is not associated with topographic forcing. At first sight it seems that the topographic component of precipitation over the Sierra in Central America be partially responsible for this precipitation maximum, but the maximum precipitation occurs where no major topographic barriers exist (see Fig. 1 and Section 2). In fact, the region just off the coast of Costa Rica and Nicaragua is relatively flat with summits around 300–400 m above sea level (see SRTM images at the site described above in Section 2). This leaves the large-scale LLJ dynamics as a plausible explanation for convective activity and precipitation maximum observed in Figure 9A. Concavity of the Central American coast and western Caribbean bathymetry may also be elements to consider, but those are beyond the scope of this work.

For February (Fig. 10A, B) the situation is slightly different; the maximum precipitation is (Fig. 10A) nearly the same as in summer (Fig. 9A), but rainfall amounts are much smaller than in the summer. The divergence–convergence patterns for winter (Fig. 10B) look similar to those of summer (Fig. 9B) but are smaller in amplitude, possibly responding to a more confined vertical structure of the IALLJ winter component (Fig. 5A). The Caribbean Sea during this season is much drier than in summer, and little convective activity is observed. Winter SSTs over the IAS are 1–2°C or more cooler than in summer, possibly preventing deep convection in an atmosphere that is frequently dried out by intrusions of cold air and associated forced convection coming from the north.

Water vapor advection by the IALLJ from the IAS into South and North America is vital to precipitation there. During the austral summer, the southern branch of the IALLJ supplies moisture to rainfall associated with the South American monsoon. In the boreal summer, the northern branch of the IALLJ, together with the GPLLJ, contributes to the humidity transport that supplies moisture to rainfall in the central United States.[111] The role of the IAS as a water vapor provider for summer rainfall in North America has been studied by many researches (e.g., Refs. 112–115 and references therein). The IALLJ at the surface is captured by scatterometer (QuikSCAT) wind data (Fig. 8A, B), and evaporation at the ocean surface is enhanced by the IALLJ structure, with intense winds extending from its maximum at 925 hPa to the surface.[48] The importance of the humidity advection by the Caribbean LLJ to regions surrounding the IAS is stressed by the result that the largest discrepancies in rainfall estimates over the continental USA in summer between the NCEP and NASA global reanalysis are directly associated with the distinction the models present when capturing LLJs.[116]

To further explore the relationship between ENSO phases and the strength of the jet core and associate these findings with precipitation patterns in the IAS, Figures 11 and 12 are presented. Using a definition of "ENSO months,"[54,117] LTM wind vector anomalies and precipitation anomalies were estimated over the IAS for July for both El Niño (Fig. 11) and La Niña (Fig. 12). Consistent with previous results for a shorter period,[54] the wind is stronger than normal during El Niño conditions over a significant portion of the IAS, including the ETP and especially in the region of the jet core (Fig. 11A). Precipitation anomalies during a warm ENSO phase (Fig. 11B) show negative values over the central Caribbean and the Pacific slope of Central America, consistent with observations. All along the Caribbean side of Central America, there are positive precipitation anomalies, in agreement with the hypothesis that precipitation maxima near

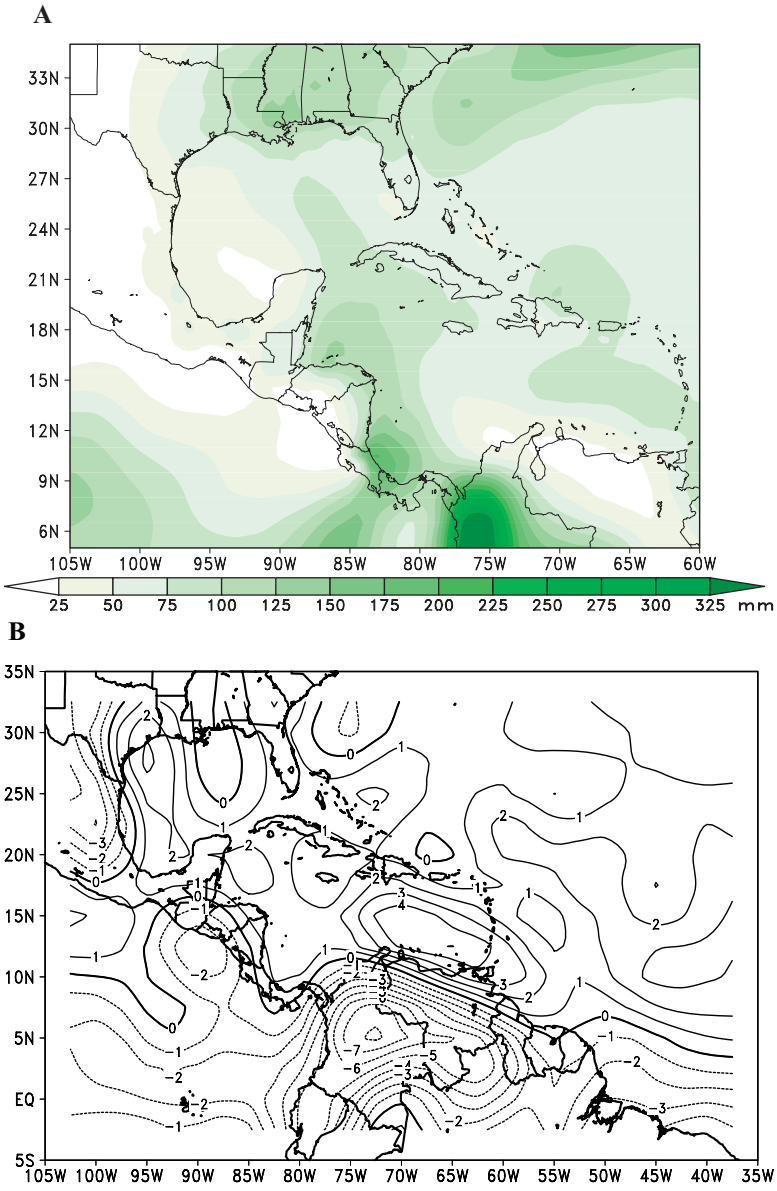

Figure 10. As in Figure 9 but for February. (In color in *Annals* online.)

Costa Rica and Nicaragua during July (Fig. 9A) and the low-level convergence–divergence patterns (Fig. 9B) are strongly associated with large-scale jet dynamics. The cold ENSO phase shows weaker than normal winds associated with the jet core for July (Fig. 12A) and negative precipitation anomalies in the western Caribbean near the Central American coasts. This finding is also in agreement with the proposed large-scale dynamic relationship between ENSO phases, the jet core strength, and precipitation anomalies over a significant part of the IAS. In other words, during a warm (cold) ENSO phase, winds associated with the IALLJ core are stronger (weaker) than normal so that precipitation anomalies are positive (negative) in the western Caribbean near Central America and negative (positive) in the central IAS

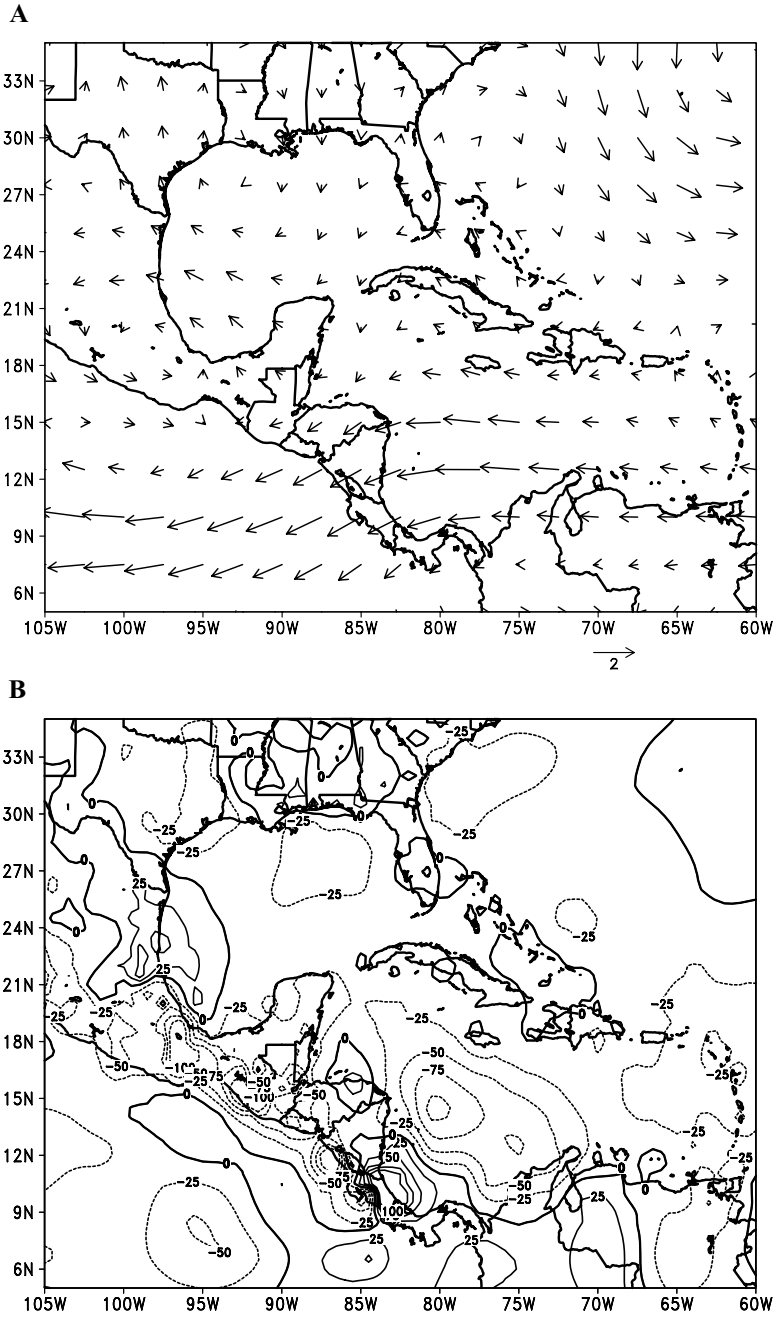

Figure 11. July long-term mean (LTM) (1958–1999) during a warm El Niño–Southern Oscillation (ENSO) event (El Niño) for **(A)** wind anomalies (m s^{-1}) at 925 hPa and **(B)** precipitation anomalies (mm).

region. How is this relationship associated with moisture advection within and outside the IAS? To answer this question, further research is required over the Caribbean. Of course there are other modulators of interannual variability of rainfall that are also significant, such as the east–west gradient of SST between the Pacific and Caribbean basins and SST anomalies

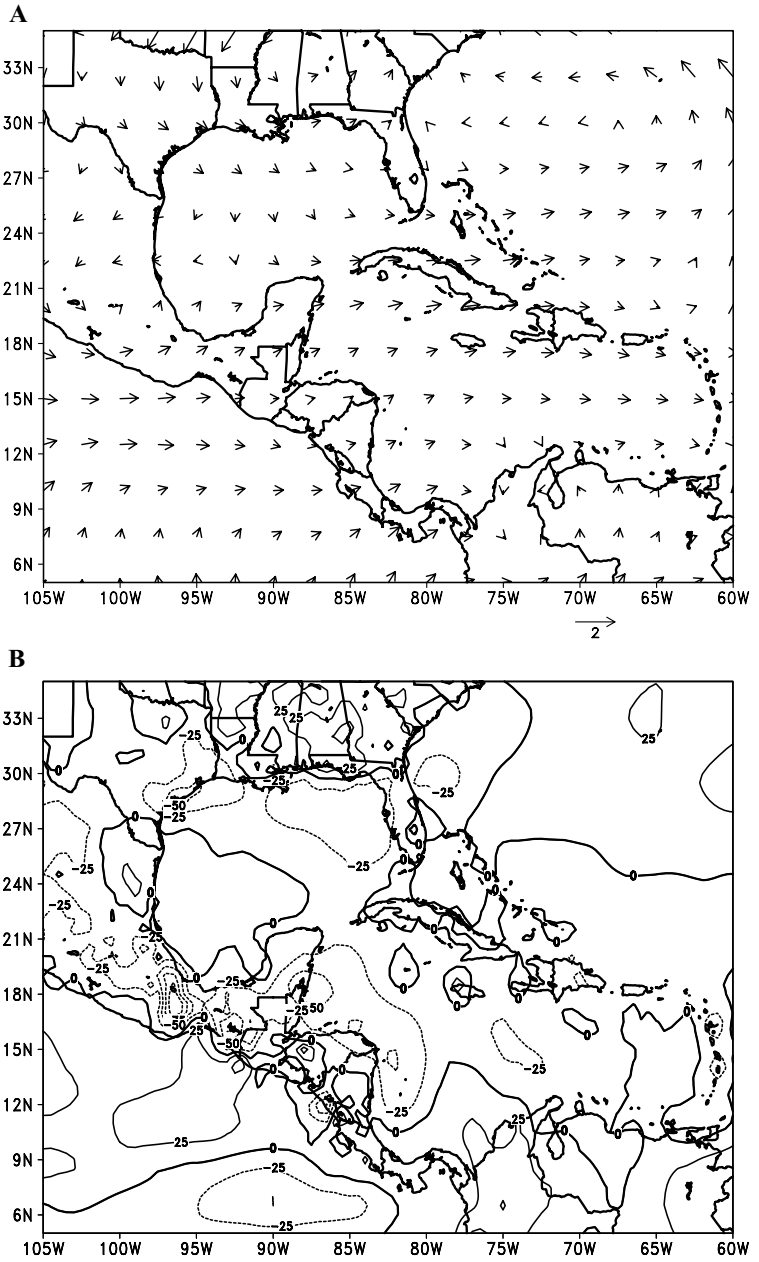

Figure 12. As in Figure 11 but for a cold ENSO event (La Niña).

in the tropical North Atlantic,[118] Caribbean SST anomalies, tropical North Atlantic sea-level pressure anomalies, vertical shear anomalies in the equatorial Atlantic, and the size of the Atlantic portion of the WHWP.[57] Although these findings look disperse, there seems to be an agreement based on scientific evidence that ENSO is the greatest single cause of interannual variability within the region, yet its effects are not universal in their timing, sign, or magnitude.[58]

The IALLJ and the CJ share common features of LLJs,[1] e.g., maximum wind speed near 1000–900 hPa, although the IALLJ is at least,

in the mean, twice as strong as the CJ. This may imply that their origin and maintenance are linked, perhaps, to quantitatively different momentum sources. The CJ has been associated with low-level moisture advection and deep-convective activity,[18] whereas the jet over the Caribbean flows in an area where lack of convection is predominant for both winter and summer in the central Caribbean. The IAS jet, in contrast to the CJ, has been shown to be barotropically unstable,[48] and it is not, as one might think, associated with any topographical feature in Central America[49,51] as its counterpart in Colombia.[18] The IALLJ and CJ are northern hemisphere features that develop during different seasons, the summer and winter for the former and autumn for the latter. Both seem to vary with ENSO episodes, but their association with warm and cold ENSO events is out of phase. During warm (cold) ENSO phases, the IALLJ during the boreal summer shows stronger (weaker) than normal wind speeds,[51] whereas the CJ presents the opposite behavior.[18]

The summer component of the IALLJ also appears to play an important dynamic role relating Caribbean and ETP SST anomalies. As discussed previously,[50,51] during warm (cold) ENSO phases, the jet shows stronger (weaker) than normal wind speeds. Fluctuations in the intensity of this LLJ then reflect in SST anomalies over the western Caribbean Sea, north of the Venezuelan coast, so that a strong (weak) jet results in negative (positive) SST anomalies over this region caused by strong (weak) Ekman transport. In this way, the jet may have a role in coupling SST anomalies in the eastern Pacific during El Niño or La Niña events with SST anomalies over some regions of the Caribbean during summer.

It has been suggested that tropical cyclone activity in the Atlantic and the Caribbean diminishes during El Niño years during the boreal summer.[119] The dynamic mechanism that controls the number of hurricanes that form over the Caribbean Sea is related to the tropospheric vertical wind shear. Another element that has been considered to play a role in this activity is the phase of the quasibiennial oscillation. The fluctuation in the intensity of the LLJ in the Caribbean (jet events) is the primary mechanism controlling the vertical wind shear amplitude during summer.[50] Anomalously warm SSTs in the eastern Pacific (El Niño conditions) result in an enhanced LLJ and therefore in a stronger than usual wind shear. During a cold ENSO phase, the LLJ weakens and the vertical wind shear decreases.[54] As a consequence of such changes in the wind shear, the number of hurricanes varies from one year to another.

How Well Do Model Simulations and Reanalysis Capture the IALLJ and Regional Circulation Features?

Figure 13[120] presents the annual cycle of the wind averaged over the area 12.5–17.5°N, 70–80°W at 925 hPa for two different model climatologies during July. As can be observed, the CCM3.6 does not capture the IALLJ at all; on the contrary, there is a decrease in the averaged wind field in July with a minimum in September. The ECHAM4.5 is closer to reanalysis but underestimates the peak if reanalysis is considered to be realistic. Both models seem to do well in capturing the strength of the winter component, but model ensembles do not necessarily give a better answer to the prediction problem in the case of the IALLJ.

A recent assessment of errors and mechanisms in the Intergovernmental Panel on Climate Change Fourth Assessment Report (IPCC AR4) on coupled ocean–atmosphere general circulation models identifies several model characteristics that need to be improved in order to gain predictability in relevant phenomena, such as ENSO and its teleconnections.[65] In the context of climate change, it is crucial to elucidate if IPCC AR4 models, in which important errors have been identified in or near the IAS,[63] can lead, realistically under global warming conditions, to a

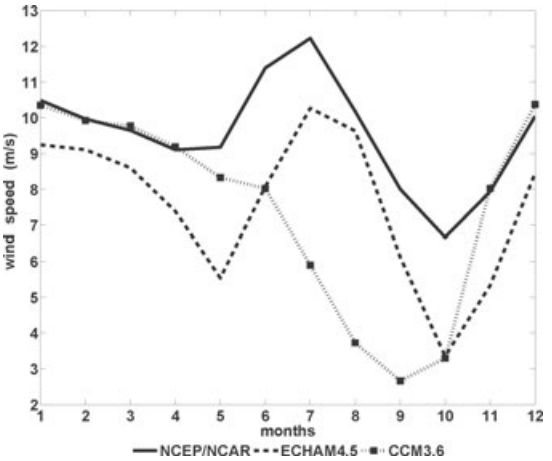

Figure 13. Annual cycle of mean wind speed (m s^{-1}) averaged over the area 12.5–17.5°N, 75–80°W for National Centers for Environmental Prediction/National Center for Atmospheric Research (NCEP/NCAR) reanalysis (*solid line*) at 925 hPa; ECHAM4.5 (*dashed line*) and CCM3.6 (*dashed-dotted line*) climatologies at 950 hPa.[120]

weakening of the tropical circulation, as has been found recently.[121] No further comments are necessary to infer all the implications that this weakening in the circulation may have in the future distribution of the IAS regional rainfall.

As is the case in most studies, reanalysis[68] has to be treated as data for the purpose of large-scale diagnostic and process studies and for validating model results. It is clear, then, that reanalysis is uncertain in data-scarce areas, such as the Caribbean. Before global reanalysis can be used to validate model simulations, the picture that has emerged of the IALLJ must first be sustained by *in situ* observations. There is, however, no aerological sounding history in the Caribbean core of the IALLJ. Uncertainties in the IAS-integrated moisture transports in the NCAR/NCEP reanalysis have been assessed and well illustrated.[115] To further exemplify problems in the reanalysis, Figure 14 is presented. Data from three stations near the Gulf of Mexico and continental United States (Monterrey, Corpus Christi, and Lake Charles) were used to compare the annual cycle of the meridional wind and moisture flux associated with the GPLLJ entrance near 30°N, using soundings and NCEP/NCAR data at those sites. Information on the stations is inserted in Figure 14. The results show evidence of a clear underestimation of reanalysis data when compared to observed data consisting of nearly 60% of the northward low-level moisture flux at Lake Charles for the period May–September. Similarly, Corpus Christi and Monterrey present underestimations of that variable on the order of 9% and 20%, respectively. The implications of these results for diagnostic, modeling, and process studies are evident. Since the selected region shows a reasonable time and spatial coverage of sounding data, contrary to what the situation is in the central Caribbean and surrounding land areas, problems associated with global reanalysis, with regard to transport of properties and water vapor estimates in the latter regions, are expected to be even larger.

ECAC Phase 3 Observations, Reanalysis, and MM5 Model Simulations

July 2001 Mean Conditions

The cold ENSO phase of 1998–2001, known as Long La Niña, was somehow average in intensity (2–3°C below normal) but long in duration. This event appeared in mid-1998 and extended approximately into early summer 2001. An ENSO-neutral mode developed after La Niña, so July 2001 was a transition month between La Niña and neutral conditions. In early 2002, El Niño phase developed. Mean sea-level pressure anomalies for July 2001 are shown in Figure 15. As observed in this figure, July 2001 does not depart too much from normal sea-level pressure; however, positive wind anomalies still persist over much of the IAS region, as in the case of a canonical cold ENSO phase. SSTs are in near normal conditions except in the Gulf of Mexico and southeastern United States (Fig. 16). In regards to the IALLJ

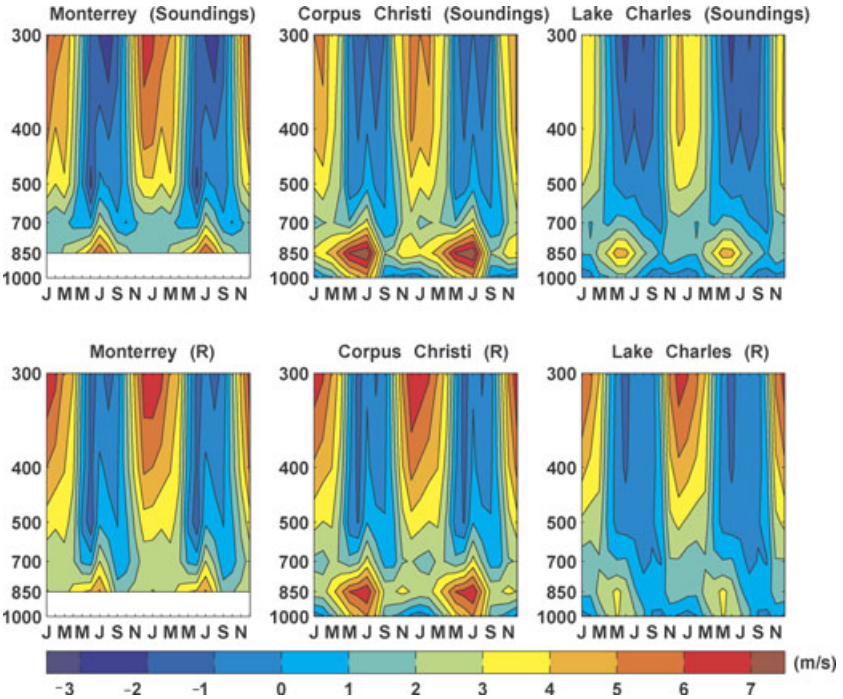

Figure 14. *Upper panels*: sounding observations at three stations (Monterrey, 25°52′N, 100°12′W, 512 m, 1973–1994; Corpus Christi, 27°46′N, 97°30′W, 13 m, 1990–2004; and Lake Charles, 30°07′N, 93°13′W, 5 m, 1973–2004, *from left to right, respectively*) near the entry to the Great Plains low-level jet (GPLLJ). *Lower panels*: NCEP/NCAR reanalysis at grid locations near the sounding stations shown in the *upper panels*. (In color in *Annals* online.)

intensity, based on the above results a weaker than normal wind structure should be expected near the jet core.

Summary of ECAC Phase 3 Weather

A short description of significant weather, especially during the main survey, follows that of Mooers *et al.*[70] The outbound phase was relatively quiet and almost free from significant weather phenomena. On July 11 Leg I commenced and the first signs of the summer component of the IALLJ were detected over the warm pool, with SSTs greater than 30°C. At the start of Leg II on July13, lightning flashes and bolts were observed in the vicinity of Jamaica. July 16 was windier and choppier, a clear signal that the vessel was approaching the northward flank of the jet. The next day, sea state was 5, and winds at deck level were in excess of 10 m s^{-1}. On July 18 the ship slowed down severely and operations were hampered by winds of 15 to 20 m s^{-1}; sea state rose to 7–8 as a result of a strong event of the IALLJ. On July 19 winds were still in the order of 10 m s^{-1} or more and reported sea state was 5–6. Winds and seas eased through the day as the ship moved away from the core of the jet and entered the warm pool to the north of the Nicaragua Ridge. Light winds and calm seas on July 20, and a fine day on July 21 were reported. The next day was also fine but cloudier, the northward extension of the IALLJ was weak, with maxima between 6 to 10 m s^{-1}. As the vessel approached Cuba on July 23, completing Leg IX and commencing Leg X, drizzle was encountered and the first (and last) rain shower of a few mm occurred; this was probably caused by the proximity to the Cuban coast and associated mid-afternoon convective activity. The

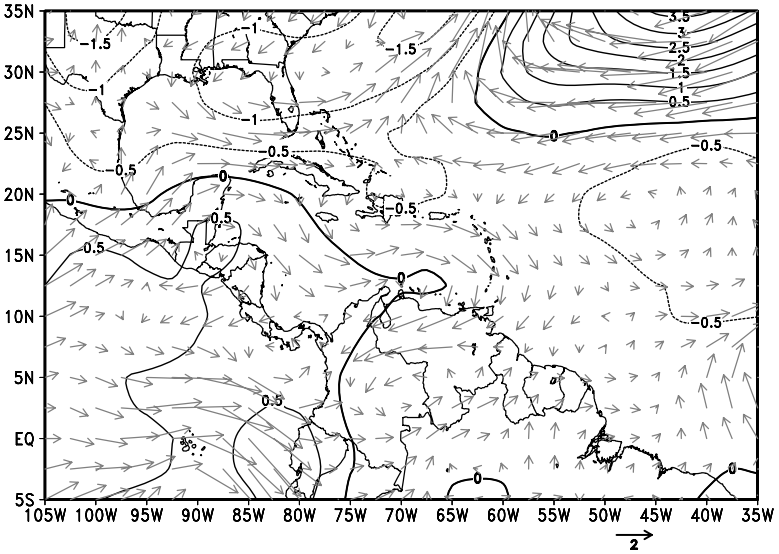

Figure 15. Sea level pressure anomalies (solid line) in hPa and wind field anomalies (gray arrows) in m s^{-1} for July 2001 at 925 hPa.

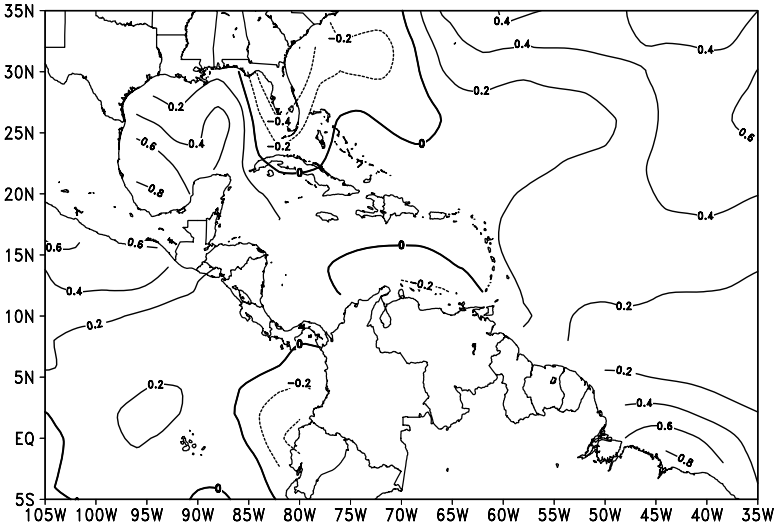

Figure 16. Long-term mean (LTM) sea surface temperature (SST) anomalies (°C) for July 2001.[72]

rest of the period for the inbound phase passed with nothing significant to report.

Observations, Reanalysis Data, and Model Results

Figure 17 presents the time variability of some meteorological parameters measured with WeatherPak instrumentation at the vessel's deck level or at the sea surface. The SST observations along the survey are shown in the top panel of Figure 17. In the northern Caribbean warm pool (July 11–14), SSTs are generally greater than 29°C with ponds of warmer water reaching 30°C or more. As the vessel moved south, SSTs decrease in the order of 1–2°C to show values of just 28°C near the surface wind maximum, just below the IALLJ core

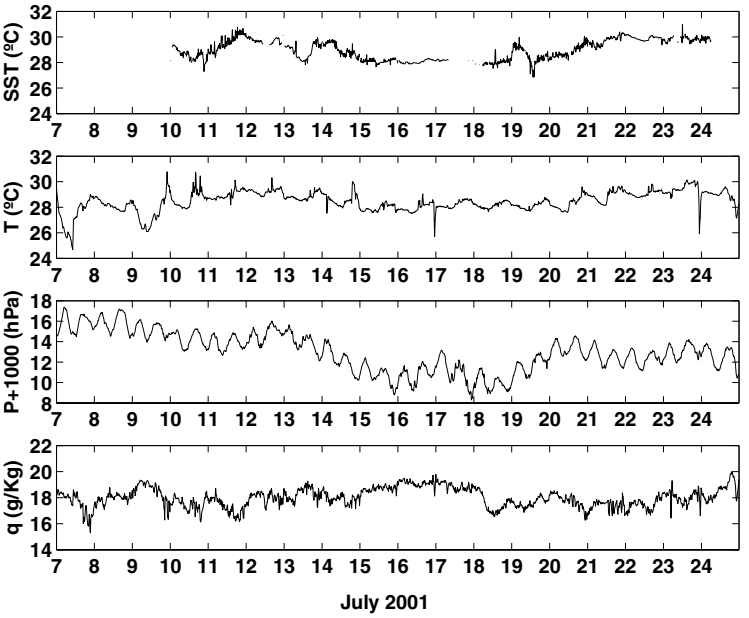

Figure 17. The 15-min averages of near-surface variables during the ECAC Phase 3 survey (July 7–24, 2001) at the R/V Justo Sierra deck level (9.5 m) for SST in °C (*upper panel*), air temperature in °C (*mid-upper panel*), pressure in hPa (*mid-lower panel*), and specific humidity in g kg^{-1} (*lower panel*).

(July 17–18). SST near or below 28°C is unfavorable for convective activity and tropical cyclone development. Under strong wind conditions upwelling develops, the marine BL is well mixed, and so SST is at a minimum when compared with nearby areas. The air temperature T (mid-upper panel) had approximately the same behavior as the SST. It is not clear if this SST minimum is well captured in available data since SST resolution in this region is a problem. As expected, pressure shows a well-marked diurnal cycle (mid-lower panel) and drops as the survey went south, except near the jet core where it increases, probably because of the effect of the strong winds (dynamic pressure) on the instruments (July 17). The specific humidity q (lower panel) was quite variable, but it sustained values in excess of 19 g kg^{-1} near the IALLJ surface maximum for several days (July 15–18).

Since one of the purposes of this work is to evaluate to what extent reanalysis captures the basic structure of the IALLJ when compared to ECAC Phase 3 observations, results from soundings are presented for three basic variables: air temperature, specific humidity, and wind speed below 600 hPa, for the selected period July 15–20, 2001, at both 00.00 and 12.00 UTC. MM5 results with assimilated data are also shown along with these variables to assess the ability of the model to resolve relevant features of the LLJ structure. The vertical profile of the wind and thermodynamic variables q and $\mathcal{T}$ from the model improved slightly when assessed with actual data (when the assimilation process with ECAC Phase 3 sounding data was carried out) compared to when the assimilation process was not involved (not shown). For comparison, the reanalysis data and MM5 results were interpolated to the nearest grid point available to the R/V Justo Sierra position. The vertical profiles of $\mathcal{T}$ are shown in Figure 18. As can be observed from this figure, the reanalysis overestimates the thermal structure of the lower troposphere before, during, and after the vessel encountered the jet core on July 17–18. In most cases reanalysis shows a warming of the atmosphere in the lower levels of more than

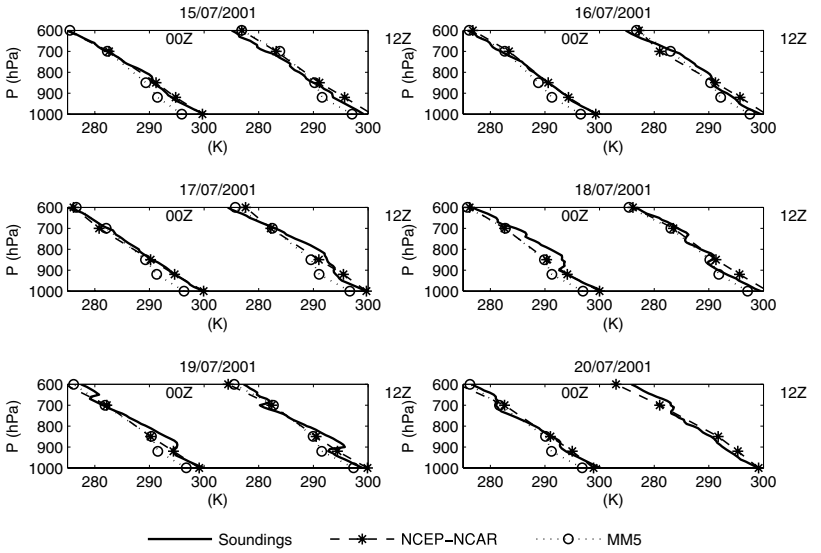

Figure 18. Vertical profiles of air temperature in °C for the period July 15 at 00.00 UTC (*upper left panel*) to July 20 at 12.00 UTC (*lower right panel*) for observations (*solid line*), reanalysis (*dots-large open circles*), and MM5 model simulations (*dashed-crosses*).

1 K and is not able to catch, perhaps as expected because of the scarcity of routine sounding data in the region, some of the low-level T inversions that are observed (e.g., July 18–19). On the contrary, MM5 shows a tendency to cool down the atmosphere, and although there is a great degree of variability in the underestimation between the ocean surface and 800 hPa, this number is in the order of 2–3 K. Figure 19 presents the vertical profile of q. A striking feature of this set of profiles is the change in the atmospheric mixed layer height (mlh) when approaching the jet core. On July 15–16, the mlh is about 100–200 m and starts to increase on the polar side of the jet (July 17 at 00.00, UTC), reaches more than 1000 m near the jet core where evaporation is at a maximum, and then decreases to 500–600 m as the vessel again returned to the polar flank of the IALLJ. This result is in qualitative agreement with July mean values of evaporation and surface fluxes (especially LHF) reported previously.[52,122]

The reanalysis and the MM5 model are not able to reproduce this important changing feature so that a proper estimation of water vapor transport toward the east or north could not be made from reanalysis for the study period. In middle levels, especially in the layer where the wind is maximum (between 800–900 hPa, see Fig. 20) or just above it, the atmosphere looked drier than expected and suggests that primary water vapor advection is taking place in a relatively shallow layer just above the surface of the ocean. The wind speed profiles are shown in Figure 20, and the evolution of the IALLJ, using *in situ* observations, is also shown for the first time. The wind maximum is observed to change dramatically in the vertical; this may be because the survey did not necessarily follow the jet core all the time. This situation can also be true for the vertical profiles of the other two variables analyzed (Figs. 18 and 19). Another aspect worth noting is that neither reanalysis nor MM5 are capable of capturing the correct vertical wind structure of the IALLJ, although the model results show a slightly improved vertical profile in some cases (e.g., July 16, 00.00 UTC; July 17, 00.00 UTC). Using findings from Figures 19 and 20, it is not hard to see why moisture fluxes are not realistically captured in numerical models in the Caribbean.

As expected, sensible heat flux is relatively small (top panel in Fig. 21) when compared with LHF (mid panel in Fig. 21). Near the

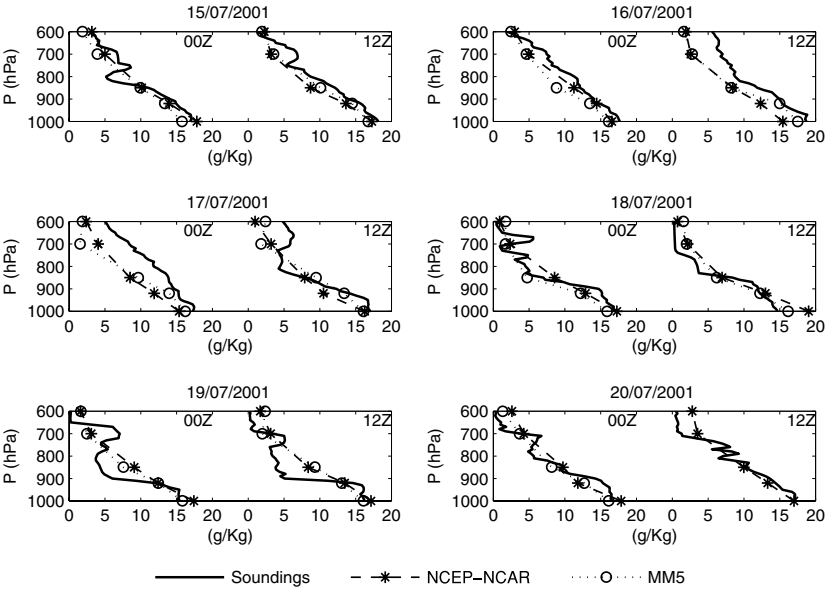

Figure 19. As in Figure 18 but for specific humidity (g kg^{-1}).

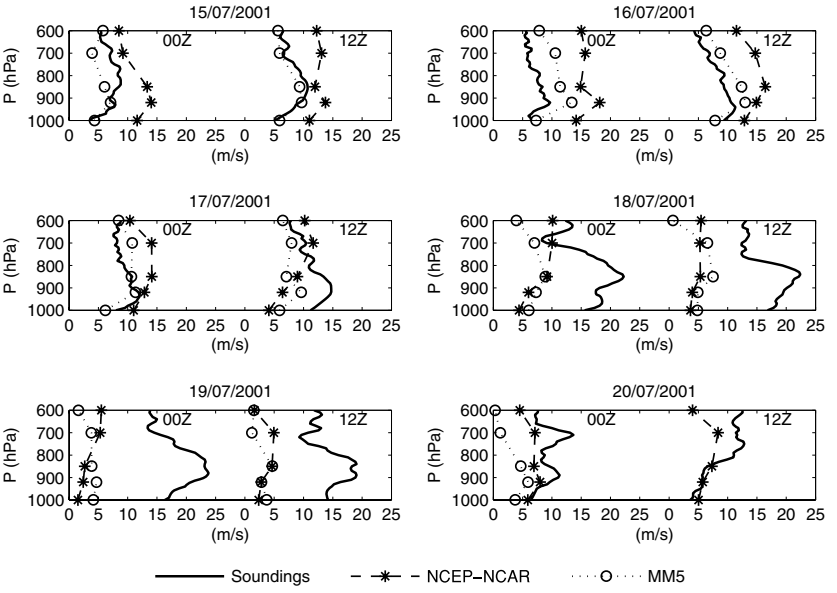

Figure 20. As in Figure 18 but for wind speed (m s^{-1}).

IALLJ surface wind maximum, sensible heat occasionally moves from the atmosphere to the ocean (e.g., July 18), with values that are usually smaller than 10 W m^{-2}. LHF presents a striking, but perhaps expected, behavior since it shows a maximum value of near 300 W m^{-2} just below the jet core. Despite the fact that strong winds tend to cool the ocean surface in the vicinity of the wind surface maximum (Fig. 17), evaporation peaks because of strong winds associated with the IALLJ, so LHF is maximum in that region. Large LHF fluctuations with peak values up to 400 W m^{-2} were observed during July 11–12 and July 22–23 in a region where the SST effect on evaporation (warm pool) predominates over the surface

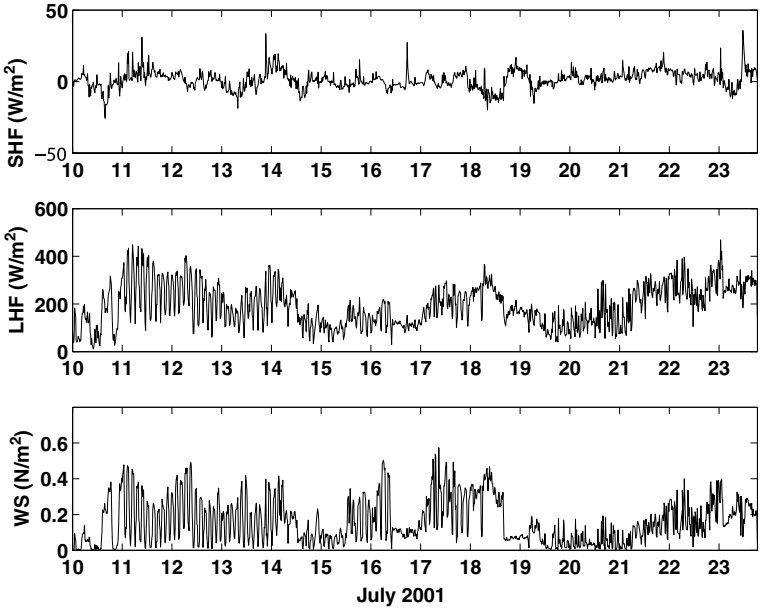

Figure 21. As in Figure 17 but for sensible heat flux in W m^{-2} (*upper panel*), latent heat flux in W m^{-2} (*middle panel*), and wind stress in N m^{-2} (*lower panel*).

wind action. As shown from the LHF distribution and considering that the survey had a north–south–north main direction, the decrease from the LHF peak on July 18 and over the following days (July 18–20) can be intuitively interpreted as a nearly northward LHF divergence component (the other may be in the nearly east–west direction). The same reasoning applies to the period July 15–18. Note that when the survey was toward the south (approximately July 11–15), LHF diminishes, the reverse being true for the period July 20–23. A possible interpretation for this estimated distribution of LHF is that the low-level flow is transporting moisture toward the north (moisture convergence). Of course, the IALLJ possibly also transports humidity toward the east to account for the precipitation maximum observed near the Costa Rican and Nicaraguan coasts. The wind stress exerted on the ocean surface (lower panel in Fig. 21) is clearly consistent with the LHF findings and confirms the relevance of local to mesoscale changes of meteorological elements in sea–atmosphere interaction processes.

Conclusions and Future Research

Atmospheric jet streams, specifically LLJs can strongly influence synoptic-scale weather systems and significantly contribute to climate through a series of dynamic mechanisms. Regional- or global-scale experiments have provided important ocean, land, and atmospheric data to study the structure and dynamics of some LLJs; however, the IALLJ of relatively recent history[48] has been less documented, despite there having been a considerable number of meteorological research programs and field campaigns covering the tropical and subtropical Americas in the last decades. The IALLJ, a relevant feature over the Caribbean Sea, lies in a region where there have been tremendous societal impacts caused by meteorological and climate systems and that is home for more than one hundred million people, many of them living in relatively small island states, some of which are among the poorest in the Americas and the world. Scientists from countries of the region have been working on the IASCLIP for execution in

the near future within the VAMOS–CLIVAR Program.

The IAS is a region with a complex topography and with a unique land–sea distribution that, to a great extent, determines its mean climate. The objectives of this paper were twofold: to update the current knowledge about the IALLJ in the context of its contribution to weather and climate in the IAS region, and to present some recent findings about the jet structure and properties based on the first *in situ* meteorological data from field work carried out during the ECAC Phase 3 campaign in July 2001. Ocean surface and atmosphere observations were used to elucidate some of the structural features of the IALLJ, and estimates of surface fluxes were made using a modern bulk formulation, COARE.[74] Standard climate data were used to complement or illustrate several relationships between the IALLJ, the MSD,[45] ENSO phases, and precipitation distribution in the region. MM5 model simulations with nonhydrostatic dynamics and standard parameterizations for the tropical oceans were used to evaluate model performance and compare results with observations and reanalysis data.

The jet shows a clear annual cycle (Fig. 4) with two wind maxima near 925 hPa, one in July and the other in January–February.[51,52,62,101,102,115] The first annual peak generally starts to develop in early June just after the onset of the rainy season in Central America, reaches a maximum in July, and then weakens in early September.[48–50] During September to early November, trades are relatively weak, vertical wind shear over the Caribbean is reduced, hurricane activity peaks, and rainfall spreads across almost all of the IAS. In late November and early December, trades increase again, cold surges from mid and high latitudes start to reach the tropics, and the second maximum of wind appears over the Caribbean Sea.[51,52,101,102] Winds in excess of 13 m s^{-1} dominate the central Caribbean Sea (15°N, 75°W) in summer where the jet core widens east–west and extends upward to 700 hPa. The winter component of the jet appears to be compressed below 850 hPa with values of up 10 m s^{-1} and with a strong vertical wind shear, an element unfavorable for convection. These differences in the strength of the IALLJ components, as observed in reanalysis data, however, should be viewed with caution since this is an area with scarce meteorological data.

The IALLJ is barotropically unstable,[48] so estimates of the barotropic energy conversions between easterly waves and the mean current, using the Elliassen-Palm flux vector, show that from May to July easterly waves lose energy and momentum, strengthening the mean current and causing a peak in the LLJ in July.[104] From August to October the IALLJ contributes with momentum to the intensification of the waves, so the jet decreases in intensity, as observed in reanalysis data.[48] The most unstable waves have phase speeds of approximately 6° per day (or 7 m s^{-1}), reach their maximum intensity at 700 hPa (contrary to African waves that peak at 850 hPa), have wavelengths of a little less than 3000 km, and have periods of 5–7 days.[104] These findings make the IALLJ an important element in explaining convective activity during the second half of the year and contributing to the understanding of regional climate; however, they are not applicable to winter when the IALLJ reaches a peak in February when no major tropical wave activity is observed.

QuikSCAT and PACS-SONET data clearly show that the low-level flow associated with the IALLJ crosses Central America and imprints the SST in the ETP. There is a striking difference in the flow configuration for summer and winter (Fig. 8). During northern summer, the LLJ splits in two branches as it passes over the Caribbean, one branch turns toward the north and the other crosses Central America and continues into the Pacific. In winter, the IALLJ turns south at the entrance of the South American subcontinent and after crossing the Central American land bridge. This large-scale circulation pattern suggests that trades, and so the IALLJ, are responding to thermal contrasts during the summer season of the corresponding

subcontinent, and it is also a natural component of the AMS. This IALLJ characteristic may also be associated with the approximate north–south distribution of land in the Americas. Since the IALLJ core intensity varies with ENSO phases in such a way that during warm (cold) events the jet core is stronger (weaker) than normal in the boreal summer, surface wind stress and wind stress curl are expected to be stronger (weaker) than in normal years in the easternmost portion of the ETP. Contrary to what happens in the summer, the jet core is weaker (stronger) than normal during warm (cold) ENSO phases in winter.[51,52] Also, strong surface winds associated with this LLJ offshore the Gulf of Papagayo influence SST over the ETP[108] and probably influence the Costa Rica dome dynamics.

The findings of this paper suggest a need to study the large-scale dynamic relationship between ENSO phases, the jet core strength, and precipitation anomalies over a significant part of the IAS. In other words, during a warm (cold) ENSO phase, winds associated with the IALLJ core are stronger (weaker) than normal, so that precipitation anomalies are positive (negative) in the western Caribbean near the Central America land and negative (positive) in the central IAS region. How is this relationship associated with moisture advection within and outside the IAS? To answer this question further research is required.

As observed during the ECAC Phase 3 field campaign, strong surface winds associated with the IALLJ induced upwelling and a well-mixed marine BL, cooling down the SST by 1–2°C. It is not clear if this minimum in SST is well captured in available data since SST resolution in this region is a problem. The specific humidity q, measured at deck level, was quite variable, but it sustained values in excess of 19 g kg^{-1} near the IALLJ surface maximum for several days (July 15–18). The reanalysis overestimates the thermal structure of the lower troposphere before, during, and after the vessel encountered the jet core on the July17–18. In most cases reanalysis shows a warming of the atmosphere at lower levels by more than 1 K and is not able to catch, perhaps as expected because of the scarcity of routine sounding data in the region, some of the low-level T inversions that are observed (e.g., July 18–19). MM5, however, tends to cool down the atmosphere, and although there is a great degree of variability in the underestimation between the ocean surface and 800 hPa, this number is in the order of 2–3 K. The atmospheric mlh changes remarkably when approaching the jet core, as described previously. The reanalysis and the MM5 model were not able to provide information to allow for a proper estimation of water vapor transport, and more *in situ* observations to test known jet theory are needed. In middle levels, especially where the wind is maximum (between 800–900 hPa, see Fig. 20) or just above it, the atmosphere appeared drier that expected and suggests that primary water vapor advection is taking place in a relatively shallow layer just above the surface of the ocean. Neither reanalysis nor MM5 were capable of capturing the correct vertical wind structure of the IALLJ, although the model results show a slightly improved vertical profile in some cases. Using findings shown in Figures 19 and 20, it is not hard to understand why moisture fluxes are not realistically captured in numerical models in the Caribbean. Sensible heat flux is relatively small with values usually smaller than 10 W m^{-2}. LHF presents a striking, but perhaps expected behavior, since it shows a maximum value of near 300 W m^{-2} just below the jet core. Despite the fact that strong winds tend to cool down the ocean surface in the vicinity of the wind surface maximum (Fig. 17), evaporation peaks because of strong winds associated with the IALLJ, so LHF is maximum in that region. A possible interpretation for this estimated distribution of LHF is that the low-level flow is transporting moisture toward the north (moisture convergence). Of course, the IALLJ possibly also transports humidity toward the east to account for the precipitation maximum observed near the coasts of Costa Rica and Nicaragua.

Several scientific questions remain to be answered. What are the dynamic mechanisms that maintain the summer and winter components of the jet? Is the IALLJ a source and/or a forcing mechanism for northward momentum and moisture transfer toward the north and east? What is the contribution of eastern Pacific summer convection in the strengthening/weakening of the IALLJ? Is the MJO involved, and, if yes, how it is associated with the intraseasonal variability of the IALLJ? Is there any relationship between the intensity (e.g., VI) of the MSD with the strength and fluctuations of the IALLJ?

Most of the presented results on the IALLJ are based on either dynamically initialized data or simulations of global models. There has not yet been a systematic study of the structure, dynamics, and variability of the IALLJ based on *in situ* observations of atmospheric soundings and field work in the IAS region.

The effort the scientific community of the VAMOS Program is making to place a Science and Implementation Plan for the IAS to study weather and climate processes (included those associated with the IALLJ) is worthy of receiving full support from international funding agencies. Quantifying systematic errors and preferences in a global model reanalysis and simulations is essential in order to improve model predictability. It is, however, reasonable to believe that present global models capture the gross features of the IALLJ and research results are credible to the first order in some cases.

Acknowledgments

This work was partially supported by the University of Costa Rica (Grants VI-805-98-506/VI-805-A7-002/VI-805-A7-755, FEEI-VI-2008) and the Inter-American Institute for Global Change Research Collaborative Research Network Grants 073 and 2050. The author expresses his deepest appreciation to his colleagues, Erick R. Rivera, A. Marcela Ulate, and Blanca Calderón for their invaluable support during the course of this work. Thanks to Luis Gimeno, Ricardo Garcia, and Ricardo Trigo, the Editors, for the opportunity to contribute to this volume. Thanks are also due to the Humboldt Chair and the Vice-Presidency for Research, University of Costa Rica, for their collaboration in carrying out this research as part of the work plan for "Catedrático Humboldt 2008."

Conflicts of Interest

The author declares no conflicts of interest.

References

1. Stensrud, D.J. 1996. Importance of low-level jets to climate. *J. Clim.* **9:** 1698–1711.
2. Bunker, A.F. 1965. Interactions of the summer monsoon air with the Arabian Sea. In *Symp. On Meteorological Results of the Int. Indian Ocean Expedition July 1965 Bombay 7–9*. Available from India Meteorological Department, Lodi Road, New Delhi-3, India.
3. Findlater, J. 1966. Cross-equatorial jet streams at low-level over Kenya. *Meteor. Mag.* **95:** 353–364.
4. Hoecker, W.H. Jr. 1963. Three southerly low-level jet systems delineated by the Weather Bureau special pibal network of 1961. *Mon. Wea. Rev.* **91:** 573–582.
5. Bonner, W.D. 1968. Climatology of the low level jet. *Mon. Wea. Rev.* **96:** 833–850.
6. Lettau, H. & K. Lettau. 1978. Exploring the world's driest climate. IES Rep. 101, Center for Climate Research, Institute for Environmental Studies, University of Wisconsin. 264.
7. Garreaud, R.D. & R.C. Muñoz. 2005. The low-level jet off the West Coast of Subtropical South America: structure and variability. *Mon. Wea. Rev.* **133:** 2246–2261.
8. Muñoz, R.C. & R.D. Garreaud. 2005. Dynamics of the low- level jet off the West Coast of Subtropical South America. *Mon. Wea. Rev.* **133:** 3661–3677.
9. Krishnamurti, T.N. 1961. On the role of the subtropical jet stream of winter in the atmospheric general circulation. *J. Atmos. Sci.* **18:** 657–670.
10. Bordi, I., K. Fraedrick, F. Lunkeit, & A. Sutera. 2007. Tropospheric double jets, meridional cells, and eddies: a case study and idealized simulations. *Mon. Wea. Rev.* **135:** 3118–3133.

11. Blackadar, A.K. 1957. Boundary layer wind maxima and their significance for the growth of nocturnal inversions. *Bull. Amer. Meteor. Soc.* **38:** 282–290.
12. Walters, C.K. & J.A. Winkler. 2001. Airflow configurations of warm season southerly low-level wind maxima in the Great Plains. Part I: spatial and temporal characteristics and relationship to convection. *Wea. Forecasting.* **16:** 513–530.
13. Walters, C.K. 2001. Airflow configurations of warm season southerly low-level wind maxima in the Great Plains. Part II: the synoptic and subsynoptic-scale enviroment. *Wea. Forecasting.* **16:** 531–551.
14. Douglas, M.W. 1995. The summertime low-level jet over the Gulf of California. *Mon. Wea. Rev.* **123:** 2334–2347.
15. Douglas, M.W., A. Valdez-Manzanilla & R. García. 1998. Diurnal variation and horizontal extent of the low-level jet over the Northern Gulf of California. *Mon. Wea. Rev.* **126:** 2017–2025.
16. Mo, K.C. & E.H. Berbery. 2004. Low-level jets and the summer precipitation regimes over North America. *J.G. R.* [DOI: 10.1029/2003JD004106].
17. Mo, K.C., M. Chelliah, M.L. Carrera, *et al.* 2005. Atmospheric moisture transport over the United States and Mexico as evaluated in the NCEP regional reanalysis. *J. Hydrometeor.* **6:** 710–728.
18. Poveda, G. & O.J. Mesa. 2000. On the existence of Lloró (the Rainiest Locality on Earth). Enhanced Ocean-Land-Atmosphere Interaction by a Low-Level Jet. *Geophys. Res. Lett.* **27:** 1675–1678.
19. Higgins, R.W., Y. Yao, E.S. Yarosh, *et al.* 1997. Influence of the Great Plains low-level jet on summertime precipitation and moisture transport over the central United States. *J. Clim.* **10:** 481–507.
20. Higgins, R.W., Y. Yao & X.L. Wang. 1997. Influence of the North American Monsoon System on the United States summer precipitation regime. *J. Clim.* **10:** 2600–2622.
21. Lackmann, G.M. 2002. Cold-Frontal vorticity maxima, the low-level jet, and moisture transport in extratropical cyclones. *Mon.Wea. Rev.* **130:** 59–74.
22. Fast, J.D. & M.D. McCorcle. 1990. A two numerical sensitivity study of the Great Plains low-level jet. *Mon. Wea. Rev.* **118:** 151–163.
23. Helfand, H.M. & S.D. Schubert. 1995. Climatology of the simulated Great Plains low-level jet and its contribution to the continental moisture budget of the United States. *J. Clim.* **8:** 784–806.
24. Ting, M. & H. Wang. 2006. The role of the North American topography on the maintenance of the Great Plains summer low-level jet. *J. Atmos. Sci.* **63:** 1056–1068.
25. International and Scientific Management Group for GATE. 1974. GATE final international scientific plans. *Bull. Amer. Meteor. Soc.* **55:** 711–744.
26. Riehl, H. 1978. Recent tropical experiments in the general context of tropical meteorology. In *Meteorology over the tropical oceans*. D.B. Shaw, Ed.: 9–30. R. Meteor. Soc. Bracknell, Berkshire, UK.
27. Reed, R.J. & E.E. Recker. 1971. Structure and properties of synoptic-scale wave disturbances in the equatorial western pacific. *J. Atmos. Sci.* **28:** 1117–1133.
28. Reed, R.J. 1978. The structure and behavior of easterly waves over West Africa and the Atlantic. In *Meteorology over the tropical oceans*. D.B. Shaw, Ed. R. Meteor. Soc. Bracknell, Berkshire, UK.
29. Gray, W.M. 1978. Their formation, structure, and likely role in the tropical circulation. In *Meteorology over the tropical oceans*. D.B. Shaw, Ed. R. Meteor. Soc. Bracknell, Berkshire, UK.
30. Higgins, R.W., A. Douglas, A. Hahmann, *et al.* 2003. Progress in Pan American CLIVAR Research. The North American Monsoon System. *Atmósfera* **16:** 29–65.
31. Higgins, R.W., J.A. Amador, A. Barros, *et al.* 2006. The North American Monsoon Experiment (NAME) 2004 Field Campaign. *Bull. Amer. Meteor. Soc.* **87:** 79–94.
32. Mo, K.C., E. Rogers, W. Ebisuzaki, *et al.* 2007. Influence of the North American monsoon experiment (NAME) 2004 enhanced soundings on NCEP operational analyses. *J. Clim.* **20:** 1821–1842.
33. Higgins, R.W. & D. Gochis. 2007. Synthesis of results from the North American monsoon experiment (NAME) process study. *J. Clim.* **20:** 1601–1607.
34. Janowiak, J.E., V.J. Dagostaro, V.E. Kousky & R.J. Joyce. 2007. An examination of precipitation in observations and model forecasts during NAME with emphasis on the diurnal cycle. *J. Clim.* **20:** 1680–1692.
35. Ciesielski, P.E. & R.H. Johnson. 2008. Diurnal cycle of surface flows during 2004 NAME and comparison to model reanalysis. *J. Clim.* In press.
36. Augstein, E.H., H. Riehl, F. Ostapoff & V. Wagner. 1973. Mass and energy transports in an undisturbed Atlantic trade wind flow. *Mon. Wea. Rev.* **101:** 101–111.
37. Holland, J.S. & E.M. Rasmusson. 1973. Measurements of the atmospheric mass, energy and momentum over 500-kilometer square of tropical ocean. *Mon. Wea. Rev.* **101:** 44–55.
38. Betts, A.K. 1973. A composite mesoscale cumulonimbus budget. *J. Atmos. Sci.* **30:** 597–610.
39. Cifelli, R., S.W. Nesbitt, S.A. Rutledge, *et al.* 2007. Radar characteristics of precipitation features in the EPIC and TEPPS regions of the East Pacific. *Mon. Wea. Rev.* **135:** 1576–1595.
40. Riehl, H. 1954. *Tropical Meteorology*. McGraw Hill. New York. 392.

41. Hastenrath, S. 1991. *Climate Dynamics of the Tropics*. Kluwer Academic Publishers. Dordrecht. 488.
42. Mapes, B., T.T. Warner, M. Xu & A.J. Negri. 2003. Diurnal patterns of rainfall in northwestern South American. Part I: observations and context. *Mon. Wea. Rev.* **131:** 799–812.
43. Schultz, D.M., W.E. Bracken, L.F. Bosart, *et al.* 1997. The 1993 Superstorm cold surge. Frontal structure, gap flow, and tropical impact. *Mon. Wea. Rev.* **125:** 5–39.
44. Schultz, D.M., W.E. Bracken & L.F. Bosart. 1998. Planetary- and synoptic-scale signals associated with Central American cold surges. *Mon. Wea. Rev.* **126:** 5–27.
45. Magaña, V., J.A. Amador & S. Medina. 1999. The mid-summer drought over Mexico and Central America. *J. Clim.* **12:** 1577–1588.
46. Wang, C. & D.B. Enfield. 2001. The tropical western hemisphere warm pool. *Geophys. Res. Lett.* **28:** 1635–1638.
47. Wang, C. & D.B. Enfield. 2003. A further study of the tropical western hemisphere warm pool. *J. Clim.* **16:** 1476–1493.
48. Amador, J.A. 1998. A climatic feature of tropical Americas. The trade wind easterly jet. *Top. Meteor. Oceanogr.* **5:** 91–102. Available at the Instituto Meteorológico Nacional (http://www.imn.ac.cr/publicaciones/index.html), San José, Costa Rica.
49. Amador, J.A. & V. Magaña. 1999. Dynamics of the low level jet over the Caribbean Sea. In Preprints 23rd. Conference on Hurricanes and Tropical Meteorology, January 10–15, 1999. *Amer. Meteor. Soc.* **2:** 868–869.
50. Amador, J.A., V. Magaña & J.B. Pérez. 2000. The low level jet and convective activity in the Caribbean. In Preprints 24th. Conference in Hurricanes and Tropical Meteorology May 29-June 2, 2000. *Amer. Meteor. Soc.* **1:** 114–115.
51. Amador, J.A., J.R. Chacón & S. Laporte. 2003. Climate and climate variability in the Arenal Basin of Costa Rica. In *Climate and Water. Transboundary Challenges in the Americas*. H.F. Díaz y B. Morehouse, Eds.: 317–350. Kluwer Academic Publishers. the Netherlands.
52. Amador, J.A., E.J. Alfaro, O.G. Lizano & V. Magaña. 2006. Atmospheric forcing of the eastern tropical Pacific. A review. *Prog. Oceanogr.* **69:** 101–142.
53. Sadler, J.C. & L.K. Oda. 1980. GATE analysis: the synoptic (A) scale circulations during phase I; Means for phases I, II and III. Department of Meteorology, University of Hawaii. UHMET 80-01.
54. Mora, I. & J.A. Amador. 2000. El ENOS, el IOS y la corriente en chorro de bajo nivel en el oeste del Caribe. *Top. Meteor. Oceanogr.* **7:** 1–20. Available at the Instituto Meteorológico Nacional (http://www.imn.ac.cr/publicaciones/index.html), San José, Costa Rica. (In Spanish).
55. Cortez, M. & J. Matsumoto. 2001. Cambios intra-estacionales en la circulación regional sobre México, Investigaciones Geográficas. *Boletin del Instituto de Geograffa, UNAM* **6:** 30–44. (In Spanish).
56. Magaña, V., J.L. Vázquez, J.L. Pérez & J.B. Pérez. Impact of El Niño on precipitation in Mexico. *Geofis. Int.* **42:** 313–330.
57. Ashby, S.A., M.A. Taylor & A.A. Chen. 2005. Statistical models for predicting rainfall in the Caribbean. *Theor. Appl. Climatol.* [DOI 10.1007/s00704-004-0118-8].
58. Poveda, G., P.R. Waylen & R.S. Pulwarty. 2006. Annual and inter-annual variability of the present climate in northern South America and southern Mesoamerica. *Palaeogeogr. Palaeoclim. Palaeoecology* **234:** 3–27.
59. Bernal, G., G. Poveda, P. Roldán & C. Andrade. 2006. Patrones de variabilidad de las temperaturas superficiales del mar en la costa caribe colombiana. *Rev. Acad. Colomb. Cienc.* **30:** 195–208 (In Spanish).
60. Kessler, W.S. 2006. The circulation of the eastern tropical Pacific. A review. *Prog. Oceanogr.* **69:** 181–217.
61. Wang, C. 2007. Variability of the Caribbean Low-Level Jet and its relations to climate. *Climate Dyn.* [DOI 10.1007/s00382-007-0243-z].
62. Wang, C. & S. Lee. 2007. Atlantic warm pool, Caribbean Low-Level Jet, and their potential impact on Atlantic hurricanes. *Geophys. Res. Lett.* [DOI:10.1029/2006GL028579].
63. Romero-Centeno, R., J. Zavala- Hidalgo & G.B. Raga. 2007. Midsummer gap winds and low-level circulation over the Eastern Tropical Pacific. *J. Clim.* **20:** 3768–3784.
64. White, F.S., M.A. Taylor, T.S. Stephenson & J.D. Campbell. 2007. Features of the Caribbean Low-Level Jet. *Int. J. Clim.* [DOI: 10.1002/joc.1510].
65. De Szoeke, S.P. & S-P. Xie. 2008. The tropical eastern Pacific seasonal cycle: assessment of errors and mechanisms in IPCC AR4 coupled ocean-atmosphere general circulation models. Accepted in *J. Clim.* **21:** 2573–2590.
66. Muñoz, E., A.J. Busalacchi, S. Nigam & A. Ruiz-Barradas. 2008. Winter and summer structure of the Caribbean Low-Level Jet. Accepted in *J. Clim.* **21:** 1260–1276.
67. Song, Q., T. Hara, P. Cornillon & C.A. Friehe. 2004. A comparison between observations and MM5 simulations of the marine atmospheric boundary layer across a temperature front. *J. Atmos. Oceanic Technol.* **21:** 170–178.

68. Kalnay, E., M. Kanamitsu, R. Kistler, *et al.* 1996. The NCEP/NCAR Reanalysis 40-year Project. *Bull. Amer. Meteor. Soc.* **77:** 437–471.
69. Douglas, M., W. Fernández & M. Peña. 1999. Design and evolution of the PACS SONET observing system in Latin America. In *3rd Symposium on Integrated Observing Systems*, January 10–15, 1999. 131–134.
70. Mooers, C., J.A. Amador, A. Gallegos, *et al.* 2001. IAI/CRN-73. R/V Justo Sierra Cruise Report, University of Miami. 15.
71. Magaña, V. & E. Caetano. 2005. Temporal evolution of summer convective activity over the Americas warm pools. *Geophys. Res. Lett.* [DOI:10.1029/2004GL021033].
72. Smith, T.M. & R.W. Reynolds. 2004. Improved extended reconstruction of SST (1854–1997). *J. Clim.* **17:** 2466–2477.
73. Gill, A.E. 1982. *Atmosphere-Ocean Dynamics*. Academic Press. New York. 662.
74. Fairall, C.W., E.F. Bradley, J.E. Hare, *et al.* 2003. Bulk parameterization of air-sea fluxes. Updates and verification for the COARE algorithm. *J. Clim.* **16:** 571–591.
75. Smith, S.R., M.A. Bourassa & R.J. Sharp. 1999. Establishing more truth in the true winds. *J. Atmos. Oceanic Technol.* **16:** 939–952.
76. Grell, G.A., J. Dudhia & D.R. Stauffer. 1995. A description of the fifth generation Penn State/NCAR mesoscale model (MM5). NCAR Tech. Note NCAR/TN-380+STR. 138.
77. Dudhia, J. 1993. A non-hydrostatic version of the Penn State–NCAR Mesoscale Model: Validation tests and simulation of an Atlantic cyclone and cold front. *Mon. Wea. Rev.* **121:** 1493–1513.
78. Riehl, H. 1979. *Climate and Weather in the Tropics*. Academic Press. London, UK. 611.
79. Wang, C. & P. Fiedler. 2006. ENSO variability in the eastern tropical Pacific. A review. *Prog. Oceanogr.* **69:** 239–266.
80. Small, R.J.O. & S.P. De Szoeke. 2007. The Central America Midsummer drought: regional aspects and large-scale forcing. *J. Clim.* **20:** 4853–4873.
81. Goldenberg, S.B., C.W. Landsea, A.M. Mestas-Nuñez & W.M. Gray. 2001. The recent increase in Atlantic hurricane activity. Causes and implications. *Science* **293:** 474–479.
82. Wyrtki, K. & G. Meyers. 1976. The trade wind field over the Pacific Ocean. *J. Appl. Meteor.* **15:** 698–704.
83. Srinivasan, J. & G.L. Smith. 1996. Meridional migration of tropical convergence zones. *J. Appl. Meteor.* **35:** 1189–1202.
84. Portig, W.H. 1976. The climate of Central America. In *World Survey of Climatology*. W. Schweidtfeger, Ed.: 405–478, Vol. 12. Climates of Central and South America Elsevier. New York.
85. Romero-Centeno, R., J. Zavala- Hidalgo, A. Gallegos & J.J. O'Brien. 2003. Isthmus of Tehuantepec wind climatology and ENSO signal. *J. Clim.* **16:** 2628–2639.
86. Vera, C., R.W. Higgins, J.A. Amador, *et al.* 2006. Toward a unified view of the American Monsoon Systems. *J. Clim.* **19:** 4977–5000.
87. Figueroa, S.N. & C. Nobre. 1990. Precipitation distribution over central and western tropical South America. *Climanálise* **5:** 36–44.
88. Mock, C.J. 1996. Climate controls and spatial variations of precipitation in the western United States. *J. Clim.* **9:** 1111–1125.
89. Holton, J.R. 2004. *An Introduction to Dynamic Meteorology*, 4d ed. Academic Press. New York. 535.
90. Schmitz, J.T. & S.L. Mullen. 1996. Water vapor transport with the summertime North American Monsoon as depicted by ECMWF analysis. *J. Clim.* **9:** 1621–1634.
91. Mestas-Nuñez, A.M., D.B. Enfield & C. Zhang. 2007. Water vapor fluxes over Intra-Americas sea: seasonal and interannual variability and associations whit rainfall. *J. Clim.* **20:** 1910–1922.
92. Maddox, R.A. 1980. Mesoscale convective complexes. *Bull. Amer. Meteor. Soc.* **61:** 1374–1387.
93. Mapes, B.E., P. Liu & N. Buenning. 2005. Indian monsoon onset and the Americas midsummer drought: out-of-equilibrium responses to smooth seasonal forcing. *J. Clim.* **18:** 1109–1115.
94. Velásquez, R.C. 2000. Mecanismos físicos de variabilidad climática y eventos extremos en Venezuela. Tesis de Licenciatura en Meteorología, Departamento de Física Atmosférica, Oceánica y Planetaria, Escuela de Física, Universidad de Costa Rica, 118. San José, Costa Rica. (In Spanish).
95. Enfield, D.B. & E.J. Alfaro. 1999. The dependence of Caribbean rainfall on the interaction of the tropical Atlantic and Pacific Oceans. *J. Clim.* **12:** 2093–2103.
96. Enfield, D.B. 1996. Relationships of inter-American rainfall to tropical Atlantic and Pacific SST variability. *Geophys. Res. Lett.* **23:** 3305–3308.
97. Enfield, D.B. & D. Mayer. 1997. Tropical Atlantic sea surface temperature variability and its relation to El Niño-Southern Oscillation. *J. Geophys. Res.* **102**(C1): 929–945.
98. Alfaro, E.J. & L. Cid. 1999. Ajuste de un modelo VARMA para los campos de anomalías de precipitación en Centroamérica y los índices de los océanos Pacífico y Atlántico Tropical. *Atmósfera* **12:** 205–222. (In Spanish).
99. Giannini, A., Y. Kushnir & M.A. Cane. 2000. Interannual variability of Caribbean rainfall, ENSO, and the Atlantic Ocean. *J. Clim.* **13:** 297–311.
100. Madden, R.M. & P.R. Julian. 1972. Description of global-scale circulation cells in the tropics with

a 40–50 day period. *J. Atmos. Sci.* **29:** 1109–1123.

101. Amador, J.A. & K.C. Mo. 2005. The Intra-Americas Sea Low-Level Jet. Poster Session 4: Hydrologic Variability and Monsoons. Song Yang, Chair. Poster 4.9 at the 30th Annual Climate Diagnostics & Prediction Workshop Climate Prediction Center, National Weather Service, The Pennsylvania State University October 24–28.
102. Amador, J.A., E.R. Rivera, A.M. Ulate & C. Zhang. 2005. The Intra-Americas Sea Low-Level Jet: An Analysis of Atmospheric Sounding Observations. Presented at Session 10: Monsoons and Warm Season Predictions. Jenni Evans, Chair. The 30th Annual Climate Diagnostics & Prediction Workshop Climate Prediction Center, National Weather Service, the Pennsylvania State University October 24–28.
103. Molinari, J., D. Knight, M. Dickinson, *et al.* 1997. Potential vorticity, easterly waves and tropical cyclogenesis. *Mon. Wea. Rev.* **125:** 2699–2708.
104. Salinas, J.A. 2006. Dinámica de las ondas del este y su interacción con el flujo medio en el Caribe. Ph. D. Thesis. Universidad Nacional Autónoma de México. México D.F. (In Spanish).
105. Chelton, D.B., M.H. Freilich & S.K. Esbensen. 2000a. Satellite observations of the wind jets off the Pacific Coast of Central America. Part I. Case studies and statistical characteristics. *Mon. Wea. Rev.* **128:** 1993–2018.
106. Chelton, D.B., M.H. Freilich & S.K. Esbensen. 2000b. Satellite Observations of the wind jets off the Pacific Coast of Central America. Part II. Regional relationships and dynamical considerations. *Mon. Wea. Rev.* **128:** 2019–2043.
107. Fiedler, P.C. 2002. The annual cycle and biological effects of the Costa Rica Dome. *Deep-Sea Res.* **49A:** 321–338.
108. Xie, S-P., H. Xu, W.S. Kessler & M. Nonaka. 2005. Air–sea interaction over the Eastern Pacific Warm Pool: gap winds, thermocline dome, and atmospheric convection. *J. Clim.* **18:** 5–20.
109. Whyte, F.S., M.A. Taylor, T.S. Stephenson & J.D. Campbell. 2007. Features of the Caribbean low level jet. *Int. J. Clim.* [DOI: 10.1002/joc.1510].
110. Granger, O. 1985. Caribbean climates. *Prog. Phys. Geogr.* **9:** 16–43.
111. Ropelewski, C.F. & E.S. Yarosh. 1998. The observed mean Annual cycle of moisture budgets over the central United States (1973–1992). *J. Clim.* **11:** 2180–2190.
112. Hastenrath, S. 1966. The flux of atmospheric water vapor over the caribbean sea and the Gulf of Mexico. *J. Appl. Meteor.* **5:** 778–788.
113. Rasmusson, E.M. 1968. Atmospheric water vapor transport and the water balance of North America. II. Large-Scale water balance investigations. *Mon. Wea. Rev.* **96:** 720–734.
114. Brubaker, K.L., P.A. Dirmeyer, A. Sudradjat, *et al.* 2001. A 36-yr Climatological description of the evaporative sources of warm-season precipitation in the Mississippi River Basin. *J. Hydrometeor.* **2:** 537–557.
115. Mestas-Núñez, A.M., C. Zhang & D.B. Enfield. 2005. Uncertainties in estimating moisture fluxes over the Intra-Americas Sea. *J. Hydrometeor.* **6:** 696–709.
116. Mo, K.C. & R.W. Higgins. 1996. Large scale atmospheric moisture transport as evaluate in the NCEP/NCAR and the NASA/DAO reanalysis. *J. Clim.* **9:** 1531–1545.
117. Trenberth, K.E. 1997. The definition of El Niño. *Bull. Amer. Met. Soc.* **78:** 2771–2777.
118. Taylor, M.A., D.B. Enfield & A.A. Chen. 2002. Influence of the tropical Atlantic versus the tropical Pacific on Caribbean rainfall. *J. Geophys. Res.* **107**(C9): 3127. [DOI:10.1029/2001JC001097.2002].
119. Gray, W.M. 1984. Atlantic seasonal hurricane frequency. Part I. El Niño and 30 mb Quasi_Biennial Oscillation influences. *Mon. Wea. Rev.* **112:** 1649–1668.
120. Rivera, E.R. 2006. El problema y aplicaciones de la reducción de escala dinámica para la predicción climática estacional en Centroamérica. Tesis de Maestría en Ciencias de la Atmósfera, Programa de Posgrado en Ciencias de la Atmósfera, Sistema de Estudios de Posgrado, Universidad de Costa Rica, 120 pp. San José, Costa Rica. (In Spanish).
121. Vecchi, G.A. & B.J. Soden. 2007. Global warming and the weakening of the tropical circulation. *J. Clim.* **20:** 4316–4340.
122. Da Silva, A., A.C. Young & S. Levitus. 1994. *Atlas of Surface Marine Data, Vol. 1: Algorithms and Procedures*. NOAA Atlas NESDIS 6, U.S. Department of Commerce. Washington, DC.